

## **TECTONIC EVOLUTION OF THE WESTERN HUDSON HIGHLANDS, NEW YORK**

JEFFREY R. CHIARENZELLI

*St. Lawrence University, Canton, NY 13617*

DAVID W. VALENTINO

*Department of Atmospheric and Geological Sciences, State University of New York at Oswego, Oswego, NY 13126*

ALEXANDER E. GATES

*Department of Earth and Environmental Sciences, Rutgers University, Newark, NJ 07102*

MATTHEW L. GORRING

*Department of Earth and Environmental Studies, Montclair State University, Upper Montclair, NJ 07043*

### **INTRODUCTION**

The New York Geological Association field conference in 2001 was organized to be run in southern New York State and northern New Jersey. Although the field guide for the conference was published by the association, the decision was made to postpone the field conference due to the attacks that took place on September 11<sup>th</sup> that year. In the end, the field trips were not run that year. Between 2001 and 2006, a considerable amount of geologic mapping was complete in the western Hudson Highlands supported by new geochronology and geochemistry, so a field excursion was prepared for the 2006 National Geological Society of America meeting held in Philadelphia (Gates et al., 2006). That field trip was canceled due to low attendance.

Over the past decade, the authors of this field guide have continued to examine the rocks of the Hudson Highlands but also in the context of the rocks exposed in the southernmost Adirondacks. This field trip is a continuation of the trip and field guide that was prepared by Gates et al. (2001) but never held. With the integration of continued bedrock mapping in the western Hudson Highlands, coupled with new geochronology and geochemistry, our objective with this trip is to provide a general tectonic overview to support other field trips on basement geology being run during this field conference. With the heavy emphasis on basement geology this year, it's worth noting that the NYSGA field conference is being run in conjunction with the annual field conference of the Friends of the Grenville.

### **LITHOTECTONIC UNITS**

Early mapping in the region of the Hudson Highlands divide the bedrock according to lithology (Dallmeyer, 1974), resulting in geologic maps of rock types, with no apparent tectonic connections. Later mapping (Gundersen, 1986), using a strategy of "lumping" rock bodies a lithologic assemblages with common tectonic affinity, resulted in the definition of lithotectonic units, or lithofacies. Applying this system of grouping lithologies by inferred tectonic association, the bedrock geology of the western Hudson Highlands, NY was remapped and recompiled for the purpose of discovering tectonic

boundaries and associations. During a decade-long field project funded by the USGS StateMap program through the New York State Museum, the following 7.5 minute quadrangles were completed as open-file reports: Sloatsburg, Theills, Monroe, Popolopen Lake, Maybrook, Cornwall and part of Greenwood Lake and Warwick. Figure 1 is a simplified version of some of the new geological maps for this region.

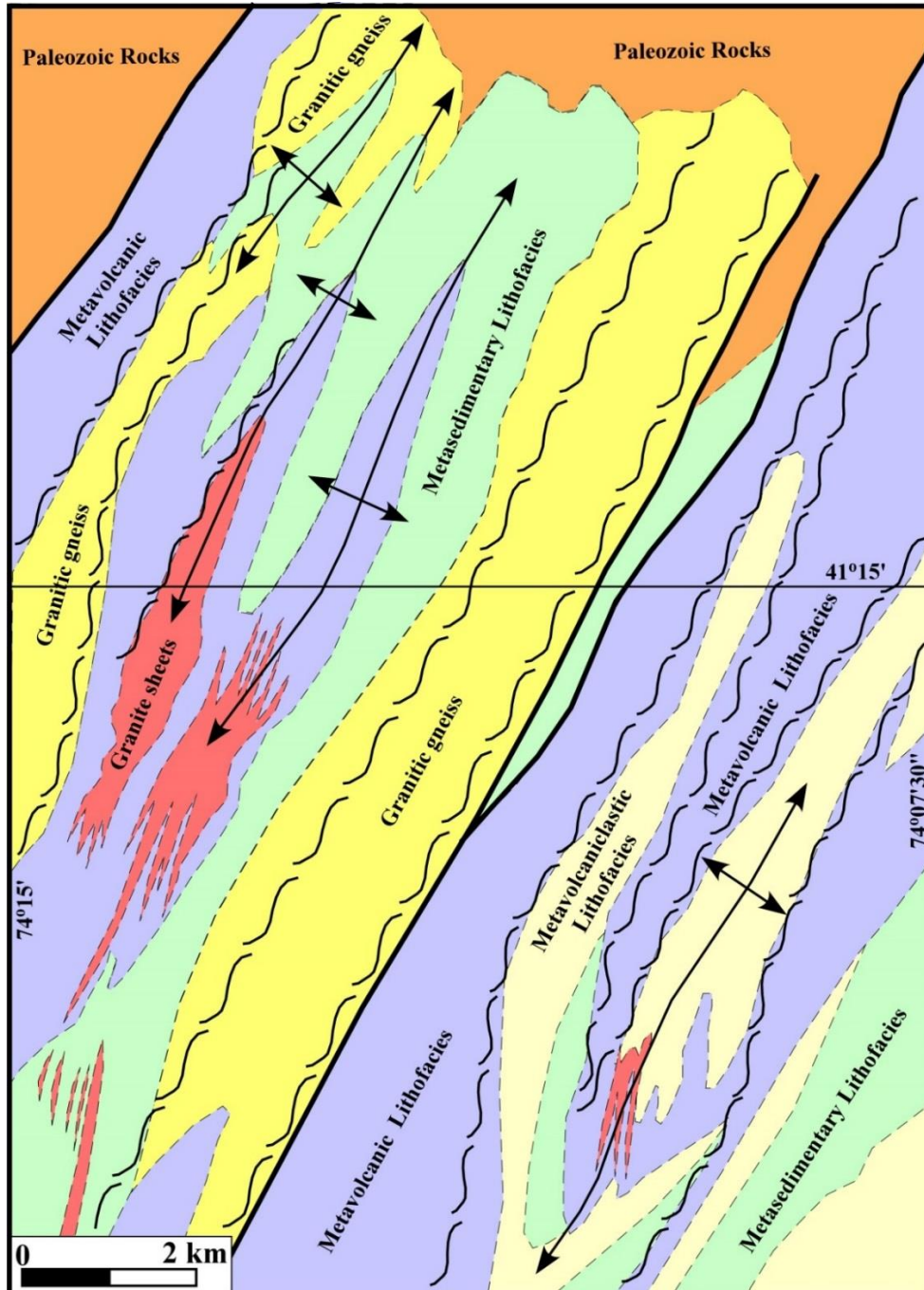


Figure 1. Geologic map of the western Hudson Highlands basement. Ductile shear zones are represented by the dashed "S" lines.

## Metasedimentary Lithofacies

The metasedimentary lithofacies includes a suite of granulite facies metamorphic rocks with protoliths that were most likely sedimentary. This lithofacies includes bodies of quartzite, minor marble, pelitic, semipelitic and psammitic gneisses (Figure 2A), and calcsilicate gneiss (Figure 2B). The meta-pelite and psammite consist of interlayered biotite-garnet gneiss with medium to coarse quartz, plagioclase, K-feldspar and local sillimanite, and cordierite with thin granitic layers. Within the metapelite are zones of graphite-pyrite-garnet gneiss with biotite, quartz, K-feldspar, plagioclase, and minor sillimanite. Some metapelites include migmatite with biotite-garnet melanosomes and thin layers of coarse granite both parallel and cross cutting the dominant gneissosity. The pelitic gneiss is often interlayered with semipelitic and psammitic gneiss and may include quartzite layers (10-50 cm thick), discontinuous layers (10-20 cm thick) of diopside and diopside-garnet marble, and calcsilicate gneiss. The calcsilicate gneiss is quartzofeldspathic with salite, apatite, sphene, scapolite, and hornblende, and is commonly migmatitic. Some calcsilicate gneiss bodies are 10's of meters thick and were mapped as separate rock bodies. All of these rock bodies are dominated by coarse gneissosity that includes intrafolial pegmatites that exhibit rootless isoclinal folding. The contacts of this gneiss body assemblage with the regional quartzofeldspathic gneiss and rocks of the metavolcanic lithofacies can be sharp or gradational.

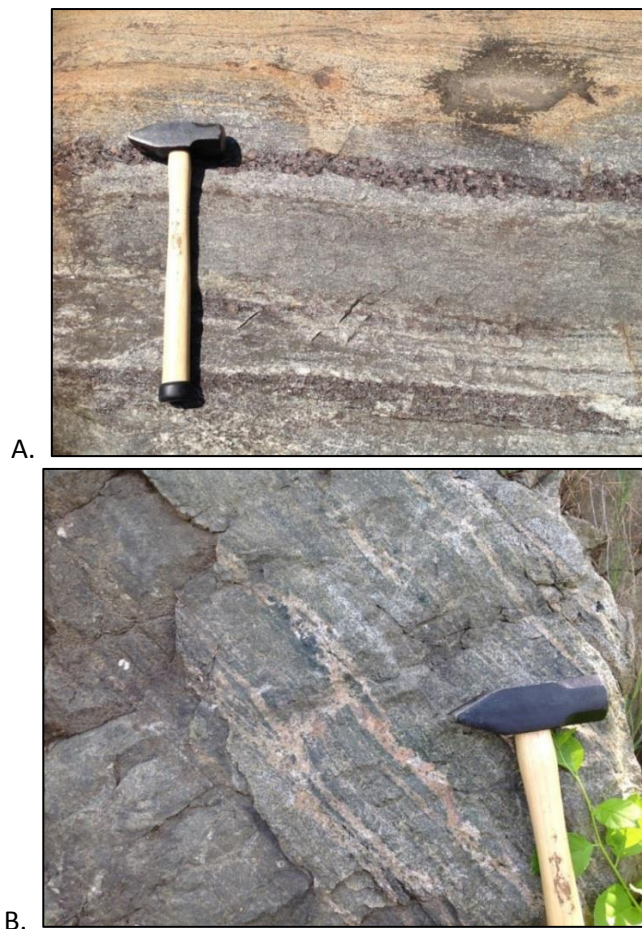


Figure 2. Photographs of metasedimentary rock outcrops. A. Psammitic gneiss with concentrations of garnet and biotite. B. Calcsilicate gneiss with K-feldspar-quartz leucosomes.

### Metavolcanic Lithofacies

The metavolcanic lithofacies includes bodies of gneiss that are made up of a mineralogically and chemically diverse assemblage of interlayered rocks at decimeter to meter scale (Figure 3). This assemblage of rocks consists of interlayered black and pale gray mafic, intermediate, and felsic gneiss. The mafic gneiss is medium to coarse grained with well-developed foliation defined by aligned augite, hornblende, plagioclase, and ortho and clino-pyroxene, and local concentrations of magnetite. The intermediate gneiss consists of medium to coarse-grained plagioclase, quartz, and minor hornblende and/or pyroxene. These two gneisses are intimately interlayered at the outcrop scale, and may include minor layers of felsic gneiss consisting of quartz, K-feldspar, plagioclase with minor hornblende.



Figure 3. Outcrop photograph of interlayered mafic, intermediate and felsic gneiss defining the metavolcanic lithofacies.

The gneissic layering ranges in thickness from 5 cm to 1.5 m with varying proportions of each rock type. Local interlayers of quartzite and calcisilicate gneiss also occur. This assemblage of rocks was inferred to have a volcanic origin, hence the metavolcanic lithofacies, based on the diverse range of rock compositions that are dominated by mafic and intermediate lithologies, and supported by being interlayered at the outcrop scale. The contacts of the metavolcanic lithofacies with metavolcaniclastic lithofacies (Figure 4) and metasedimentary lithofacies rocks are generally gradational but can be sharp locally.

### Metavolcaniclastic Lithofacies

About 30% of the western Hudson Highlands is underlain by medium to coarse grained quartzofeldspathic gneiss (Figure 4). The gneiss is characterized by massive to layered quartz-plagioclase aggregates with minor amounts of biotite, and/or hornblende, and trace magnetite, K-

feldspar, or garnet. Compositional layering in the gneiss is defined by the proportion of mafic minerals. Gates et al. (2001) reported on some layering containing gradual increase in mica with sharp contacts possibly representing original sedimentary compositional variation. In places, the quartzofeldspathic gneiss contains layers of amphibolite that are parallel to compositional layering and pervasive foliation. Locally the gneiss is interlayered with quartzite and amphibolite layers near the contacts with the metasedimentary and metavolcanic lithofacies bodies, respectively. A second foliation is directly associated with steeply dipping km-scale ductile shear zones that are well developed in the quartzofeldspathic gneiss. Commonly small pockets of granite occur between foliation boudins in the gneiss. The unit is also host to cross cutting pegmatites ranging from decimeter to several meters thick. Based on the mineral composition and the occurrence of compositional layers in the quartzofeldspathic gneiss, the unit is interpreted to represent a sequence of volcanoclastic metasedimentary rocks.



Figure 4. Outcrop photograph of strongly foliated quartzofeldspathic gneiss with an amphibolite layer.

### Granitic gneiss

In the westernmost blocks of the Hudson Highlands, there are multiple northeast striking bodies of granitic gneiss that are greatly impacted by steeply dipping ductile shear zones and are considered mylonites (Figure 1). Although mineralogically similar to the quartzofeldspathic rocks, these rocks contain relict plutonic textures such as megacrysts of plagioclase and K-feldspar that form asymmetric augen that form rotated porphyroclasts. Additionally, these granitic gneiss bodies do not contain the compositional layering that is so prominent. To characterize the geochemistry of the granitic gneiss

body, a suite of samples was collected where the body is exposed on Route 17A. As might be expected, the granitic gneisses have a relatively limited range in major oxide and trace element chemistry. For example, SiO<sub>2</sub> content ranges from 64.54 to 71.87% which is quite silicic. Details of the geochemistry are described below.



Figure 5. Outcrop photographs of granitic gneiss of the western Hudson Highlands. A. Strongly foliated course grained gneiss with minor leucosome where the foliation is disrupted. B. Course grained granitic gneiss with relict megacrysts of K-feldspar that form both symmetric and asymmetric augen.

## Granite Sheets

There is a suite of granite sheets that are concordant to the local foliation, and appear to have intruded all of the units previously described (Figure 1). The sheets range in thickness from 5 to 50 m and are laterally continuous for several kilometers. The granite is generally medium to coarse grained, locally megacrystic, and the margins of the sheets contain mylonitic foliation that is concordant with the adjacent rock bodies (Figure 6). The granite sheets commonly contain xenoliths of the local country rock. Where the granite is mylonitic, the contact with the quartzofeldspathic gneiss is difficult to determine. Although there are a few exceptions, most of the granite sheets occur in the hinge regions of km-scale upright folds in the western Hudson Highlands (Figures 1). Based on these field relations, it was concluded that the granite sheets were intruded during deformation (Thomas et al., 2001; Linguanti et al., 2011).

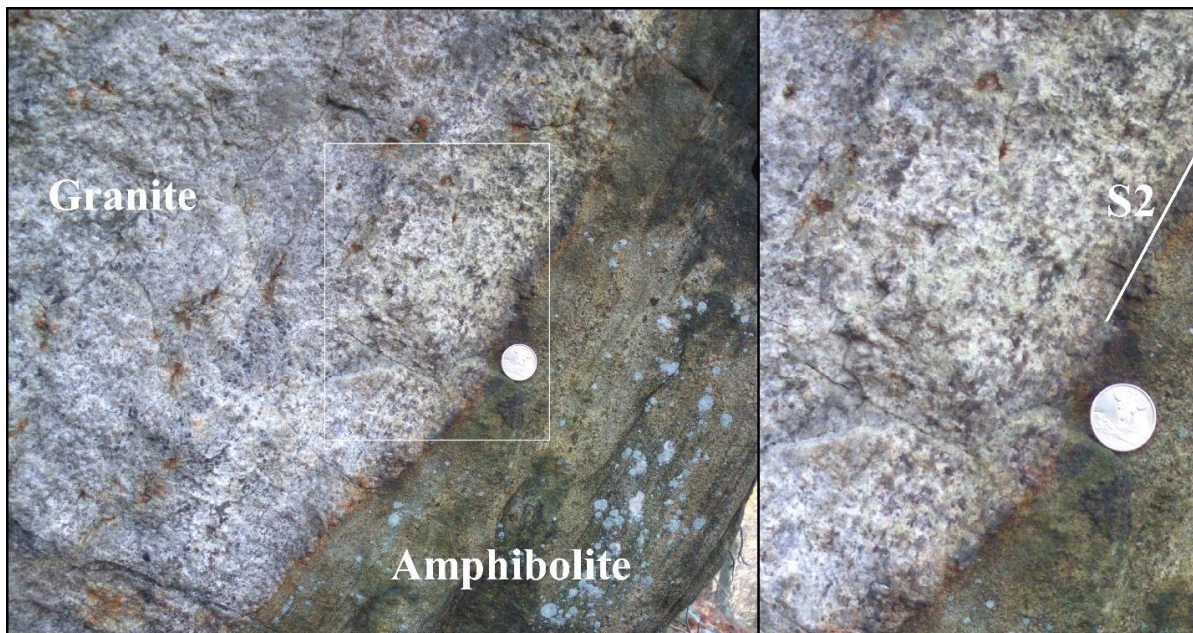


Figure 6. Photograph of the contact between the granite sheet at Tiger Hill and the local amphibolite. Note the weakly developed foliation in the margin of the granite that is parallel to the S2 foliation in the amphibolite.

## Lake Tioroti Diorite

Coarse- to very coarse-grained black and white speckled diorite contains plagioclase, pyroxene, hornblende, and biotite locally. The diorite grades to lower pyroxene, anorthositic compositions locally. Texture ranges from granoblastic to foliated and mylonitic with S-C fabric. The diorite locally contains xenoliths of country rock with ductile contacts that are partially melted to form a rind of coarse to pegmatitic granite around them and filling fractures in the diorite. The primary occurrence of this diorite is on the west shore of Lake Tioroti, and based on cross cutting relations and occurrence of local xenoliths, the diorite was used to determine the relative, and absolute age, of igneous activity and regional metamorphism and deformation (Figure 7).

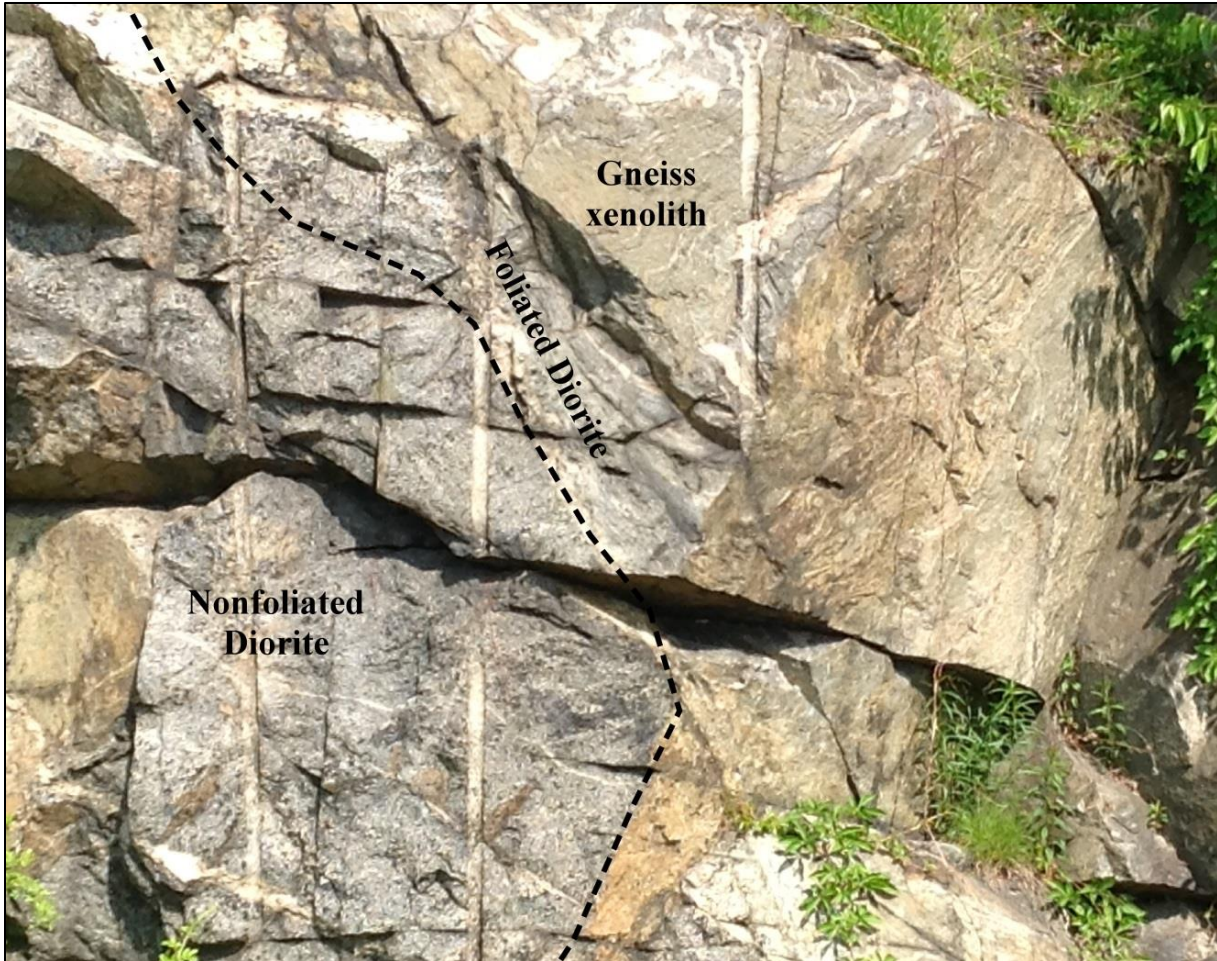


Figure 7. Outcrop photograph of Lake Tioroti diorite where it contains a xenolith of foliated gneiss (presumed to be S1 foliation) and also contains mylonitic foliation (S2) associated with the local dextral shear zone (D2).

### Pegmatites

There are two generations of pegmatite dikes in the western Hudson Highlands. Early dikes are white and contain white K-feldspar, quartz, muscovite, and garnet locally. They are largely parallel to subparallel gneissic foliation, display boudinage and contain internal foliation and plastically deformed grains. Their thickness ranges from 10cm to 1m. A second suite of pegmatite dikes cross-cut the pervasive regional foliation and foliation associated with ductile shear zones (Figure 8). These late pegmatite dikes are very coarse grained with pink K-feldspar, quartz, and locally muscovite, magnetite, pyroxene, titanite, and/or garnet, and occasionally contain elongate hornblende aggregates that define a magmatic lineation or are plumose. These pegmatites are highly discordant, commonly associated within zones of brittle shear, and contain xenoliths of fault rocks. They exhibit no internal deformational fabric, and the thickness ranges from 1m to 10m.



Figure 8. Outcrop photograph of the contact between quartzofeldspathic gneiss and a hornblende pegmatite. The geochronology for both of these units is discussed below.

## DEFORMATION AND METAMORPHISM

The basement rocks of the western Hudson Highlands experienced at least two major deformational events accompanied by emplacement of igneous bodies and high-grade metamorphism. All of the major rock units described above contain a penetrative foliation (S1) that is parallel to compositional layering and includes intrafolial isoclinal and sheath folds (F1). This foliation is defined by planar aggregates of recrystallized minerals and the pervasive gneissosity is associated with this foliation. Depending on the bulk composition, minerals such as biotite, amphibole, sillimanite, and/or pyroxene are aligned in the strongly foliated quartz-feldspar matrix. Stillwell (2005) reported on garnet-biotite exchange thermometry with temperatures ranging from 650-800°C for pelitic gneiss samples collected across the entire western Hudson Highlands. These results are consistent with the presence of sillimanite, K-feldspar, biotite and locally cordierite.

Small pegmatite bodies are commonly parallel to subparallel to the gneissosity and exhibit well developed pinch and swell, and are locally asymmetric relative to the foliation. Aggregates of hornblende and pyroxene define porphyroclasts, and rocks containing intrafolial asymmetric isoclinal folds that exhibit vergence that is consistent locally. Mesoscopic and megascopic folds are recumbent and shallowly reclined. They are tight to isoclinal and commonly asymmetric with missing lower limbs. Although the attitude of the foliation and intrafolial folds were impacted by later deformation, the overall asymmetric fold consistency suggests northwestward nappe-like ductile flow during the first deformation event. The sparse kinematic indicators described above are consistent with the vergence of folds.

Overall, the S1 high grade metamorphic fabric has a variable orientation across the western Hudson Highlands due to map-scale folding (F2) associated with younger km-scale transcurrent shear zones (Figure 1). One of the map-scale F2 folds occurs at the southern end of Lake Tiroti and another excellent example occurs in the region southwest of Sterling Lake. Both of these map-scale folds are developed in the transition zone to the large ductile shear zones.

The second deformational event is characterized by a system of subvertical to steeply dipping, northeast striking anastomosing ductile shear zones (Figure 1). These shear zones cross cut and have transposed the foliation of the first deformational event. They range from 0.5 to 2 km in thickness though the boundaries exhibit wide strain gradient in some areas and are difficult to determine. The shear zones are developed in all of the major lithotectonic units and are defined by well-developed S-C mylonite with shallowly northeast plunging mineral lineations defined by recrystallized aggregates of feldspar, quartz and/or mafic minerals. Although the shear zones cross cut all lithotectonic units, they are best developed the granitic gneiss and the quartzofeldspathic gneiss of metavolcaniclastic lithofacies.

The Lake Tiroti diorite and the granite sheets also locally contain minor S-C mylonite, indicating that the diorite and granite bodies intruded before or during the development of the D2 shear zones. Kinematic indicators within the mylonite include C-S fabric, rotated porphyroclasts, shear bands, and asymmetric boudins. There are well-developed mesoscopic sheath folds with shallow northeast plunge, and megascopic drag folds adjacent to the main shear zone. Additionally, there are highly attenuated upright folds that occur within the shear zone foliation and many exhibit a small amount of granite that was intruded parallel to the fold limbs.



Figure 9. Outcrop photograph of granitic gneiss within the Indian Hill shear zone. The view is looking down into the ground at subvertical foliation that exhibits asymmetric boudins consistent with dextral shear. The end of the hammer handle is pointing approximately 035.

Kinematic analysis was conducted on all of the segments of shear zone within the anastomosing network, and the results are consistently dextral. Minerals within the sheared rocks include amphibole and biotite as well as quartz and feldspar, all of which show plastic deformation but with full recovery, suggesting that the shear zones initiated under a minimum of amphibolite metamorphic conditions.

Meso- and macroscopic gentle to open upright folds also occur adjacent to the shear zones locally (Figures 10 and 11). These folds plunge gently from due north to north-northeast. The folds occur in well-layered metavolcanic and metasedimentary sequences directly adjacent to the shear zone boundary. In the area of Harriman State Park, upright folds form an en-echelon array with the hinge axes oblique to the north relative to the northeast strike of the shear zones. In the Sterling Forest region of the westernmost Hudson Highlands, there are upright map-scale folds defined by the map pattern of the local metasedimentary and metavolcanic rocks. The hinge regions of these upright folds are also the locations where granite sheets are most prevalent, and they are subparallel to the fold hinges, similar to observations at the outcrop described above. The granite sheets have variably developed mylonite at the contact with highly sheared country rock, suggesting syn-kinematic emplacement in the hinge of the upright folds.

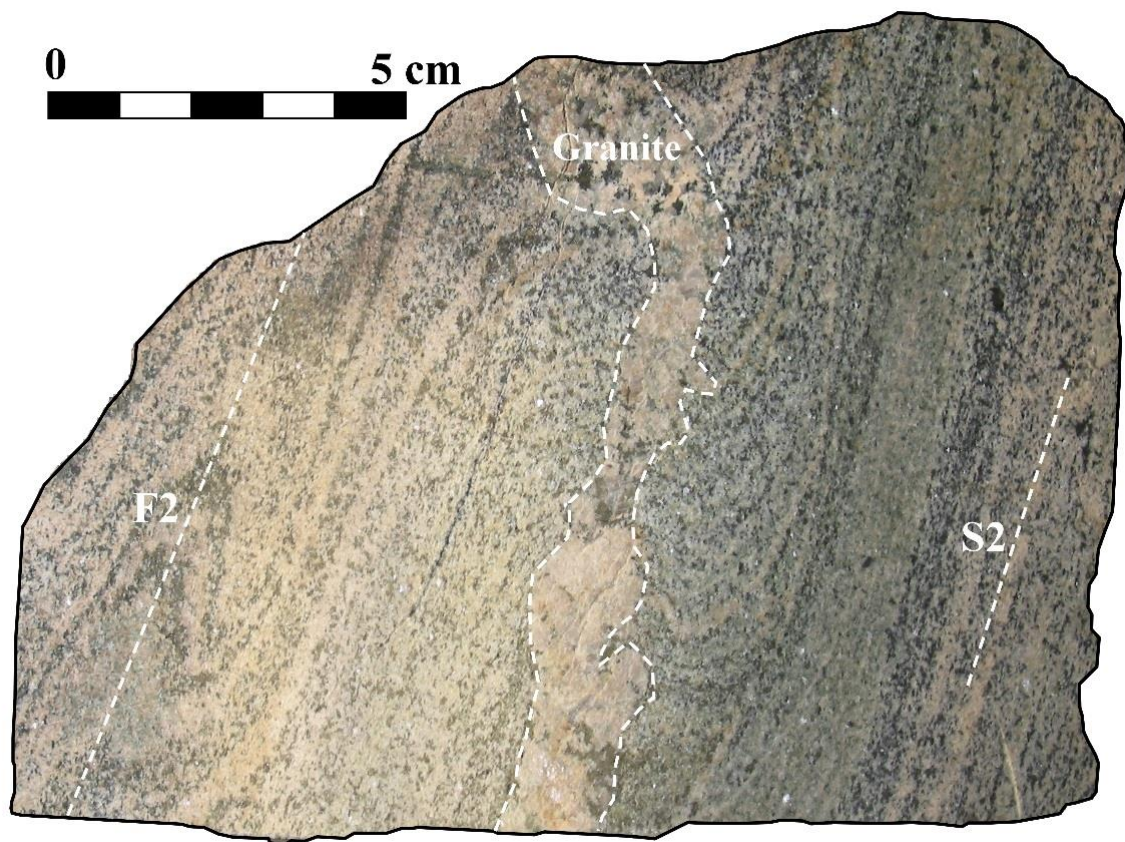


Figure 10. Cut slab of quartzofeldspathic gneiss exhibiting F2 folds and small F2-parallel granite. This is a small-scale example of the structural emplacement of the granite sheets into upright folds formed between the dextral shear zones.

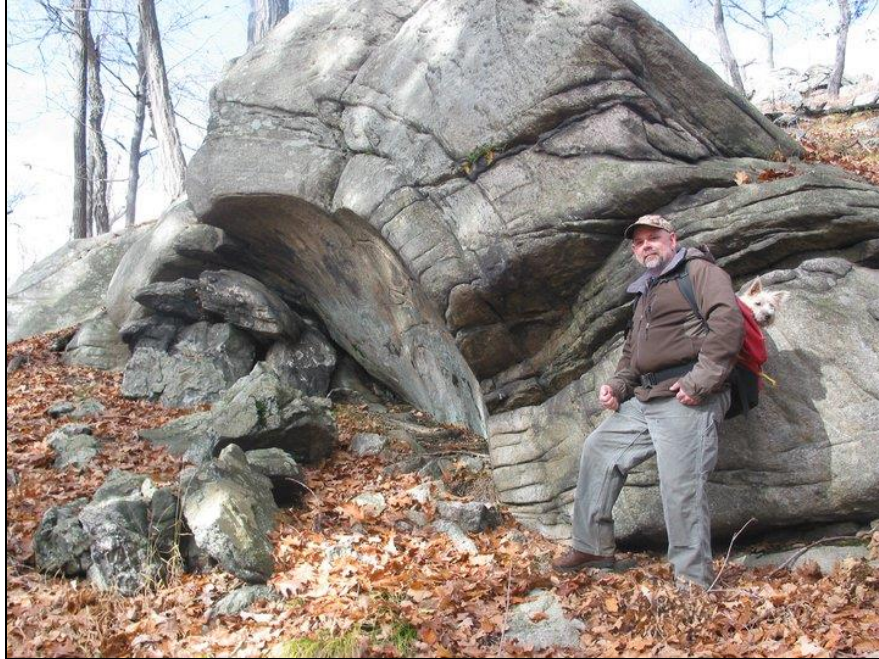


Figure 11. Upright open antiformal fold developed in quartzofeldspathic gneiss. The hinge axis of this fold is oriented oblique to the local Fingerboard shear zone (Gates and Valentino, 2011).

Late stage concordant to slightly discordant brittle fracture zones occur within several of the D2 mylonite zones and are highly mineralized. They contain randomly oriented, coarse to megacrystic intergrowths of salite and phlogopite followed by magnetite and scapolite and cemented by calcite in areas of marble. Other zones contain hornblende and clinopyroxene followed by magnetite that are contained within quartz. Zones that connect the magnetite deposits are thinner and typically composed of randomly oriented to aligned clinopyroxene with only minor magnetite, phlogopite and/or quartz. They are commonly intruded by late pegmatites that contain mineralized rock as xenoliths. Thicknesses of the zones range from 2 m to 15 m. Some of the mineralized zones are more than 5 km long and occur along the length of the ductile shear zone. The veins parallel the zones but clearly cut the mylonitic foliation with ragged to planar contacts.

## GEOCHRONOLOGY

### Metasedimentary Lithofacies

Semi-pelitic gneiss. Zircon separated from a semi-pelitic gneiss are rounded and average about 125 microns in diameter. In back scattered electron mode small rounded to oval cores, often displaying oscillatory zoning, are within much larger areas of diffuse or unzoned zircon rims. The uranium content of 13 cores averages  $613 \pm 520$  ppm and the U/Th ratios are  $3.24 \pm 1.82$  ppm. The rims of 22 grains averaged  $1487 \pm 872$  ppm and the U/Th ratios were  $57.2 \pm 50.6$ . The grains range of 95.1 to 102.4% concordant.

Figure 12 shows all of the data points plotted on a concordia diagram. Grains range in age from 2041-991 Ma. Several distinct clusters or groupings of analyses occur and Figure 3c gives the weighted means for several possible groupings which yield ages of  $1331 \pm 10$ ,  $1030.5 \pm 2.5$ , and  $1005.9 \pm 4.6$  Ma. Similar values were obtained for concordia plots and concordant ages. The wide distribution of ages suggests that the semi-pelitic gneiss is of supracrustal origin. However, BSE images suggest thick metamorphic rims have grown on or replaced the bulk of the volume of detrital grains. Similar conclusions were reached for zircon from the Irving Pond quartzite in the Adirondack Highlands analyzed by Peck et al. (2013). For comparison, relatively intact detrital zircons were found by Chiarenzelli et al. (2015) in upper amphibolite facies quartz-rich metasedimentary rocks from the Adirondack Lowlands.

Based on age, U-content, U-Th ratios, and core versus rim relations the zircon spots analyzed can be separated into those thought to yield detrital versus metamorphic ages. The youngest clearly detrital analysis has a  $^{207}\text{Pb}/^{206}\text{Pb}$  age of  $1264 \pm 12.7$  Ma and provides a maximum age for deposition of the precursor of the semi-pelitic gneiss. This age agrees well with existing geochronological information from rocks of the Grenville Supergroup including the Franklin Marble. However, the relatively small number of analyses in this study ( $n = 35$ ) limit the degree of confidence in this and other interpretations.

A cluster of 7 grains yielding an age of  $1331 \pm 10$  Ma matches well with tonalitic arc magmatism known many areas in the Grenville Province and Grenville rocks in Appalachian inliers, and are perhaps part of the Dysart-Mt. Holly Suite. Cluster ages of  $1030.5 \pm 2.5$  and  $1005.9 \pm 4.6$  Ma agree well with estimates of late Ottawaan metamorphism (see sample G-2) and late intrusion (see sample G-1) in the Hudson Highlands.

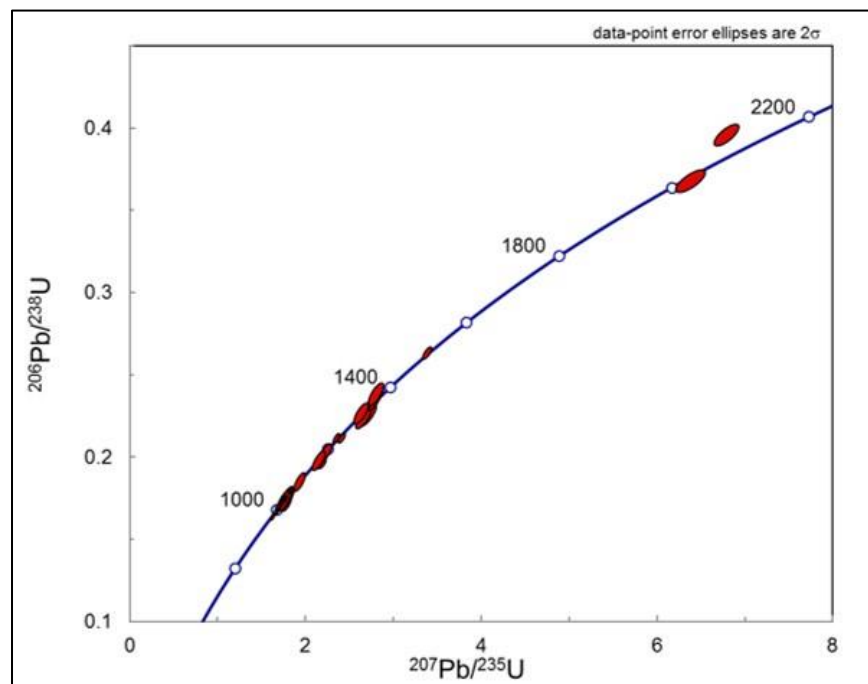


Figure 12. Concordia diagram for zircons analyzed from semi-pelitic gneiss.

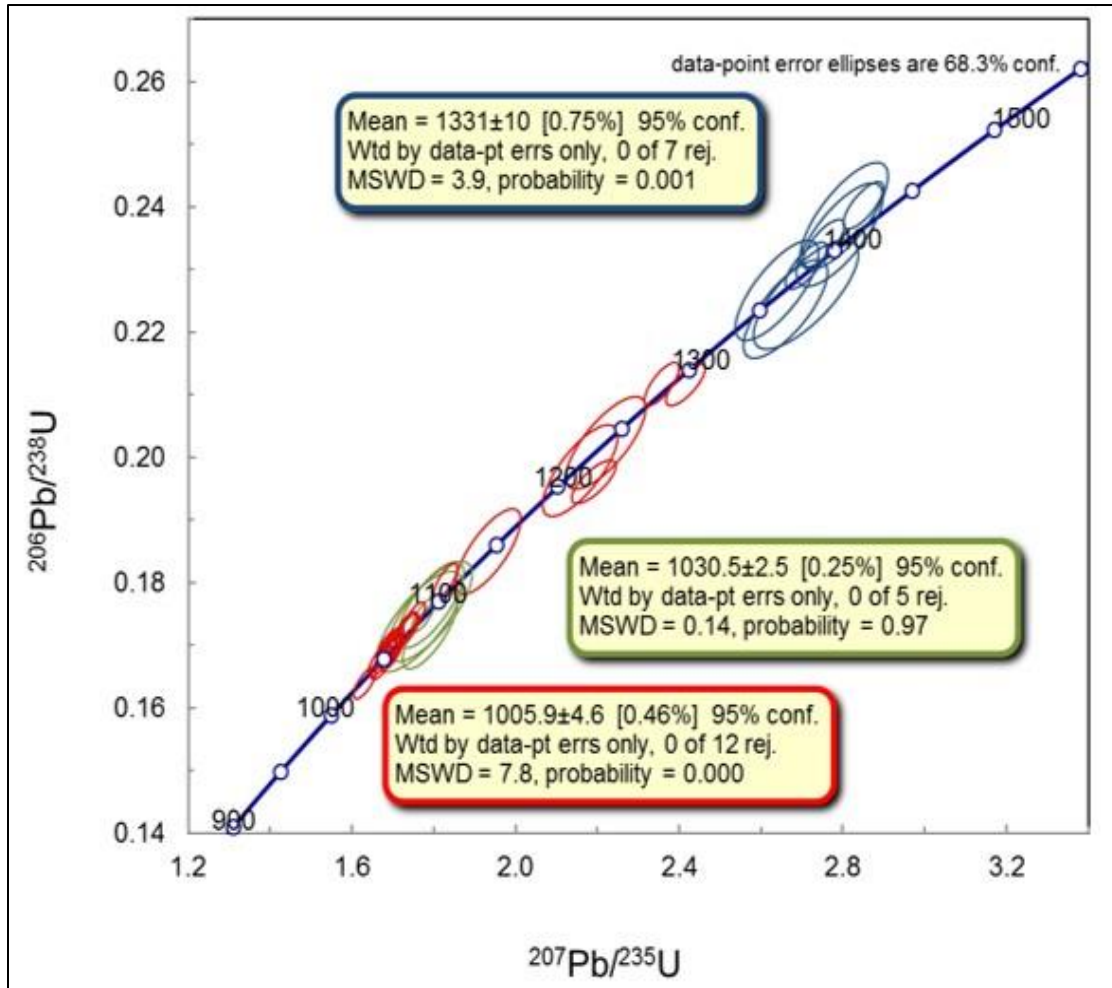


Figure 13. Geochronological results from sample G-5 a semi-pelitic gneiss located near Mombasha Lake. This enlargement of the younger analyses showing possible groupings based on the clustering of data point. Color coded ellipses correspond to results of weighted mean calculation. The two younger groupings ( $1030.5 \pm 2.5$  and  $1005.9 \pm 4.6$  Ma) are interpreted as metamorphic. The oldest grouping shown in the diagram ( $1331 \pm 10$  Ma) is believed to represent a population of detrital material derived from tonalitic rocks equivalent to Dysart-Mt. Holly Suite.

**Quartzite.** Zircons separated from a sample of quartzite have complex shapes varying from euhedral to faceted to rounded. Some grains occur as clusters and/or with other zircons nucleated off them. The majority of grains are somewhat rounded, dipyrmaid crystals about 150 microns in length. When viewed in cathodoluminescence mode several types of zoning, cores, rims, and considerable variation in brightness (i.e. CL response) is observed (Figure 14A). The uranium content of the grains is highly variable ranging from 99-1544 ppm, as is their U/Th ratios which range from 0.85-172.0. The grains range from 70 to 168% concordant. After filtering for concordancy values between 95-105%, of the 92 grains analyzed, only 49 analyses are considered suitable for further consideration. Collectively these characteristics indicate a detrital origin for the vast majority of analyses and considerable post-depositional disturbance of U-Pb isotopic systematics.

Figure 14B shows all of the data points plotted on a probability histogram. Analyses yield ages ranging from  $2749 \pm 10$  to  $960 \pm 8$  Ma. A variety of small “peaks” and several distinctive gaps in the data occur between 2052 and 2606 Ma and 1226-1303 Ma on the calculated histogram. The first gap indicates a lack of a later (ca. 2100-2500 Ma) Paleoproterozoic source. The second gap is believed to represent detrital ages from those of metamorphic or hybrid age. Analyses in the age range 1800-1500 Ma dominate the population, indicating a source(s) of this range. Curiously both Shawinigan and Ottawa ages are poorly represented, indicating few metamorphic grains or rims were analyzed, perhaps because of the preferential targeting of grain cores.

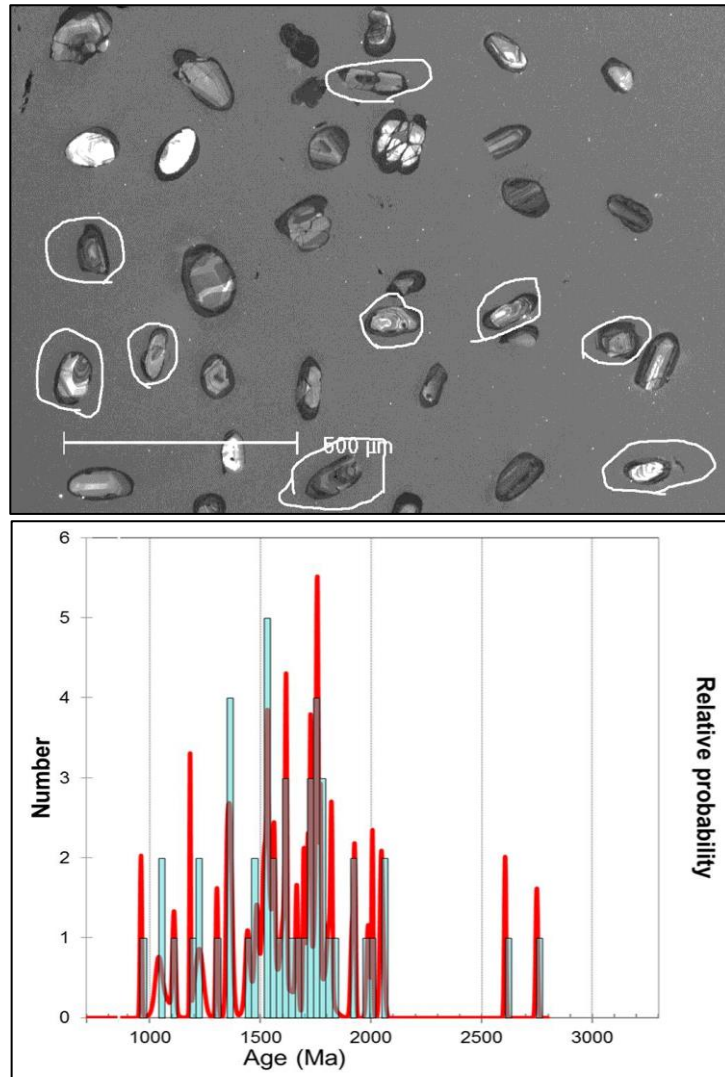


Figure 14. Geochronological results from a quartzite taken from the supracrustal sequence near Bear Mountain. A total of 49 analyses are displayed. A. Cathodoluminescence (CL) image of typical zircon grains separated from the quartzite. Note variety in shape, zoning types, and cathodoluminescence response. Grains outlined in white were selected for analysis. B. Probability histogram shows the range of ages from analyses of zircons from the quartzite. Note large gaps between Archean and Proterozoic time. Ages younger than 1303 Ma are interpreted metamorphic or hybrid (see text).

In comparison with the semi-pelitic gneiss, zircons from the quartzite appear to better represent original detrital populations, with far fewer analyses that are likely of metamorphic origin. Similar findings were noted by Chiarenzelli et al. (2015) who attributed the preservation of more detrital grains a function of the minimal reactivity and melting of high-grade quartzose rocks compared to those of pelitic origin. While the relatively small number ( $n = 49$ ) of usable detrital ages prohibits detailed interpretation of potential source(s), those of significance include a small Neoproterozoic component and various Meso- to Paleoproterozoic components, particularly those ranging in age from 1800-1500 Ma. Also present are a significant amount of ca. 1350 Ma grains thought to be derived from Dysart-Mt. Holly terrane equivalents. The youngest grain interpreted as detrital gives an age  $1303 \pm 10$  Ma providing a maximum depositional age for the quartzite.

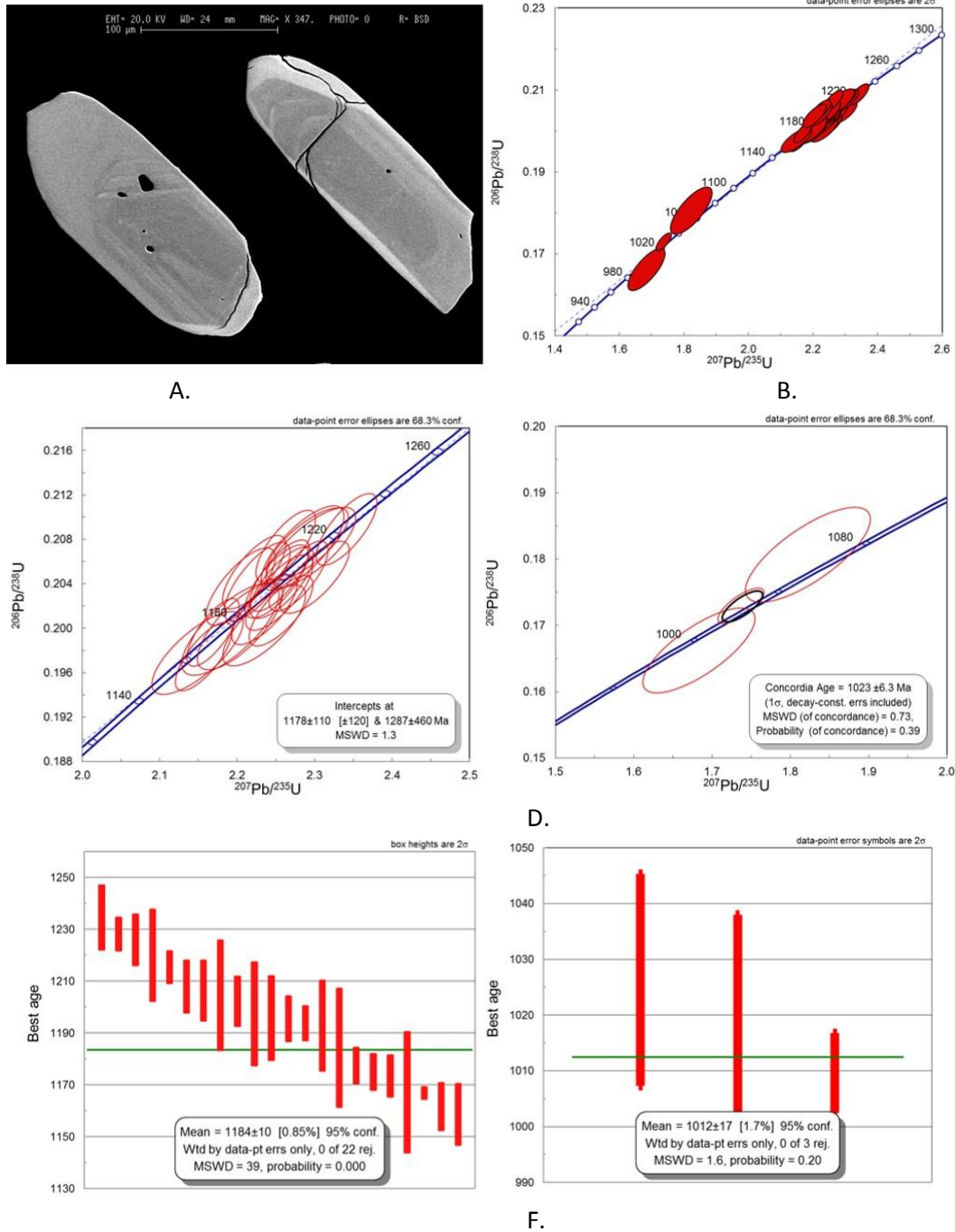
### Granitic gneiss

Zircon separated from a granitic mylonite from the Indian Hill shear zone (Allers et al., 2001) averages approximately 200 microns in length, forming modified euhedral prisms (Figure 15A). In back scattered electron mode dark zoned and rounded cores are overgrown by partial to complete, bright rims up to tens of microns across at their widest point. Fine and wide oscillatory zoning is visible in the cores. The uranium content of the cores averages  $588 \pm 514$  ppm and the U/Th ratios are very consistent at  $2.46 \pm 0.71$ . In total 22 grains and grain fragments were analyzed and yielded data points ranging from 96.4 to 103.4% concordant. The uranium content of rims average is high, averaging  $1565 \pm 107$  ppm and the U/Th ratios were  $13.7 \pm 6.4$ . In total, 3 bright rims were analyzed and yielded data points ranging from 96.6-105.1% concordant.

Figure 15B shows all of the data points plotted on a concordia diagram. Two distinct clusters occur and yield  $^{207}\text{Pb}/^{206}\text{Pb}$  ages at least 126 Ma apart and hence were grouped accordingly. In addition, distinct differences in BSE response, U content, and U/Th ratios were noted between the two groupings. The older, upper group of 22 analyses yields  $^{207}\text{Pb}/^{206}\text{Pb}$  ages between 1235 to 1159 Ma. A Concordia plot (Figure 15B) yields a lower intercept of  $1178 \pm 110$  Ma (MSWD of 1.3). A weighted mean of  $1184 \pm 10$  Ma is considerably more precise but with an MSWD of 39 unlikely to accurately represent the age of the zircons in this group.

Alternatively, the spread of analyses along concordia is likely the result of disturbance within the Indian Hill Shear Zone. High-grade mylonitic rocks deformed and metamorphosed shortly after or during their intrusion can display zircon arrays that fan out along concordia indicating continued growth or Pb-loss over an extended period. Later or recent Pb-loss can further add further complexity to zircon arrays by causing additional Pb-loss along steeper chords. We conclude that granitic rocks that form the protolith to those in Indian Hill Shear Zone where intruded shortly before metamorphism and deformation associated with the Shawinigan Orogeny, considered to have occurred between 1210-1150 Ma. Exactly when requires additional research but their time of crystallization is constrained by the  $^{207}\text{Pb}/^{206}\text{Pb}$  ages of the oldest and youngest core analyses of 1235 to 1159 Ma.

Analysis of the three bright rims yields a concordant age of  $1023 \pm 6.3$  Ma with an MSWD of 0.73. A weighted mean of  $1012 \pm 17$  Ma with an MSWD of 1.6 agrees within analytical error (Figures 15E and 15F). These results are believed to reflect the timing of late zircon growth likely associated with the latest stages of the Ottawa Orogeny (1090-1020 Ma).



E. F. Figure 15. Geochronological results from sample G-2 a quartzofeldspathic gneiss from the Indian Hill Shear Zone. A. BSE images of typical zircon grains separated from the quartzofeldspathic gneiss. B. Concordia diagram showing all U-Th-Pb analyses performed on zircons and their clustering into two major groupings. C. Blow up of the upper, older group of analyses showing both their spread along concordia and above and below it. D. Blow up of the lower grouping of three grains showing their concordant age (black circle). E. Weighted mean of the upper grouping, not the wide spread of ages and high MSWD not indicative of a single population. F. Weighted mean of the lower grouping.

Lake Tiorati Diorite

Zircon separated from the Lake Tiorati diorite average approximately 150 microns in long dimension, are primarily equant, and show faint zoning (Figure 16A). Some are euhedral showing square cross-sections; others appear to be fractured fragments of larger grains. Their uranium content averages  $463 \pm 159$  ppm and the U/Th ratios are very consistent at  $2.60 \pm 1.32$ . In total, 18 grains and grain fragments were analyzed and yielded data points ranging from 97.5 to 103.2% concordant. For these reasons the zircons are considered of igneous origin having been derived from crystallization from an intermediate to mafic magma. Little or no evidence of metamorphic rims, grains, or resetting was noted.

Plotting all 18 grains analyzed on a standard Concordia diagram yield an upper intercept age of  $1004 \pm 12$  Ma (MSWD of 0.32). A concordant age calculated from the same data set yielded an age of  $1006.8 \pm 5.0$  Ma (MSWD of 0.027; Figure 16B). A weighted mean calculated from the same data set yielded an age of  $1008.1 \pm 4.6$  Ma (MSWD of 4.5; Figure 16C). All three methods of calculating the age of the zircons from the Lake Tiorati diorite yield ages within analytical error of each other. The concordant age of  $1006.8 \pm 5.0$  Ma is taken as the time of crystallization. Thus the rock crystallized approximately 1007 Ma and the zircons have retained relatively closed U-Th-Pb isotopic systems since.

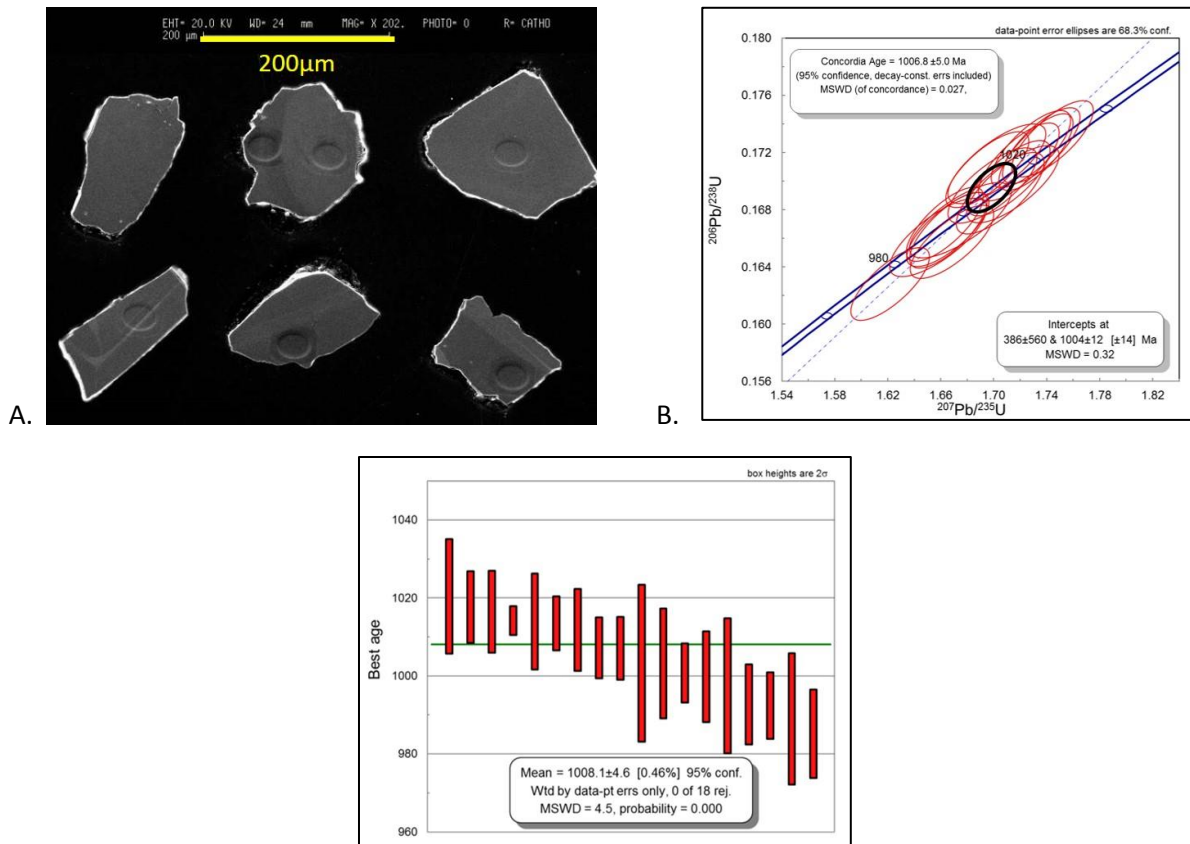


Figure 16. Geochronological results from sample G-1 Lake Tiorati Diorite. A) BSE images of typical zircon grains and fragments separated from the Lake Tiorati diorite. Note SHRIMP ablation pits. B) Concordia diagram showing all U-Th-Pb analyses performed on zircons and their clustering. The black circle outlines the calculated concordant age derived from all the analyses. C) The weighted mean calculated from all U-Th-Pb analyses of zircon.

Pegmatite

Zircons were separated from one of the larger pegmatite bodies that cross cuts the mylonitic foliation of the Indian Hill shear zone. The zircon uranium content averages  $362.4 \pm 287$  ppm and the U/Th ratios are very consistent at  $2.87 \pm 0.93$ . In total, 12 grains and grain fragments were analyzed and yielded data points ranging from 94.8 to 104.2% concordant. For these reasons, the zircons are considered of igneous origin having been derived from crystallization from a granitic magma. Little or no evidence of metamorphic rims, grains, or resetting was noted.

Plotting all 12 grains analyzed on a standard Concordia diagram yield an upper intercept age of  $990 \pm 17$  Ma (MSWD of 0.72). A concordant age calculated from the same data set yielded  $981.6 \pm 3.5$  Ma (MSWD of 2.5). A weighted mean calculated from the same data set yielded an age of  $992 \pm 14$  Ma (MSWD of 0.72). All three methods of calculating the age of the zircons from the pegmatite yield ages within analytical error of each other. The concordant age of  $981.6 \pm 3.5$  Ma is taken as the time of crystallization. Thus the rock crystallized approximately 980 Ma and the zircons have retained relatively closed U-Th-Pb isotopic systems since.

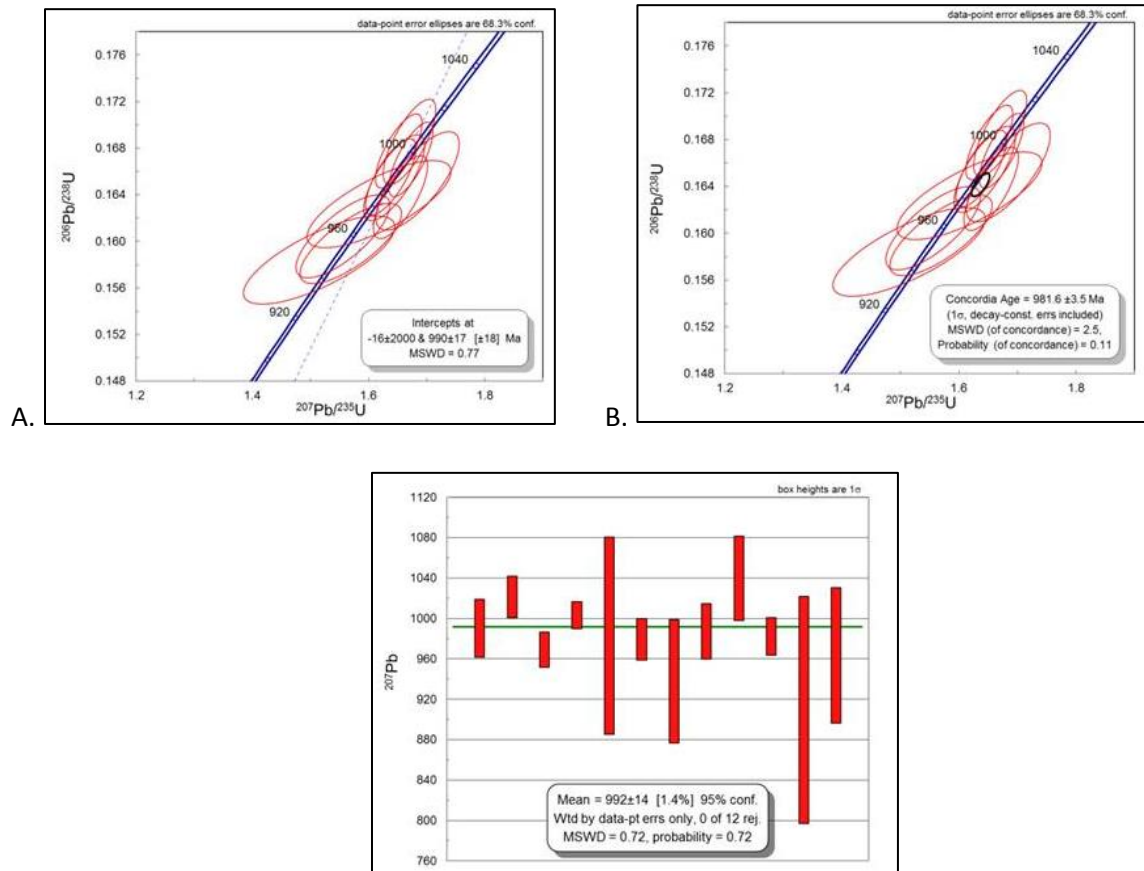


Figure 17. Geochronological results from a sample of hornblende pegmatite that cross cuts the Indian Hill shear zone along Route 17A. A total of 12 analyses are displayed. A. Cathodoluminescence (CL) image of typical zircon grains separated from the pegmatite. B. Concordia diagram showing all U-Th-Pb analyses performed on zircons and their clustering. C. A concordant age calculated from the U-Th-Pb analyses represent by the black circle. D. The weighted mean calculated from all U-Th-Pb analyses of zircon.

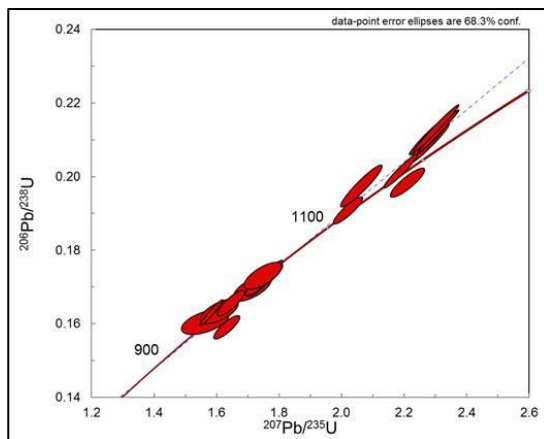
## Mineralized Zone

Zircon separates from a magnetite vein within one of the mineralized zones exhibit several different distinct morphologies and sizes, including high U cores, low-U rims, and large clear zircon grains. Their uranium content ranges between 135.5 to 2731 ppm and the U/Th ratios between 1.87 and 11.6. In total, 21 grains and grain fragments were analyzed and one was eliminated from further consideration because of its concordancy of only 90%. Two general clusters or groupings of ages can be seen on the concordia diagram (Figure 18A). In detail, several fairly coherent groupings were identified. The interpretation of the ages is equivocal.

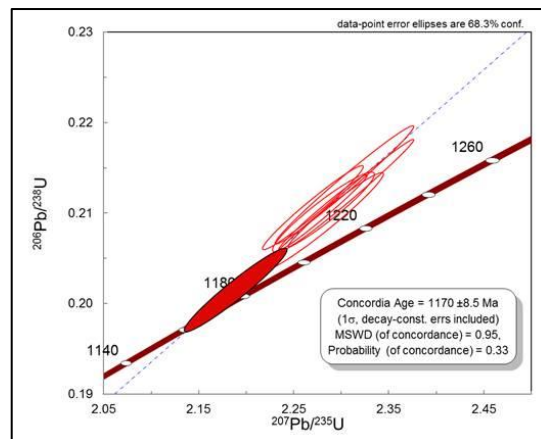
A single analysis of a core yielded a  $^{207}\text{Pb}/^{206}\text{Pb}$  age of  $1217.2 \pm 15.6$  Ma and is reasonably interpreted as a xenocrystic zircon (Figure 18B). Seven, high-U, grain cores, six of which plotted slightly above concordia yielded a concordia intercept of  $1164.5 \pm 7.2$  Ma with an MSWD of 1.4 (Figure 18B). If the single most concordant grain of the grouping is used to calculate a concordant age an analytically indistinguishable age of  $1170 \pm 8.5$  Ma with an MSWD of 0.95 is obtained.

A grouping of six slightly discordant, lower U rims, in the lower cluster yielded an upper intercept age of  $1026.8 \pm 4.3$  Ma with a MSWD of 2.5 (Figure 18A). A weighted mean calculated from the same six grains yields an analytical indistinguishable age of  $1037 \pm 14$  Ma (MSWD of 0.17). A final grouping of grains yielded a weighted mean of  $949 \pm 31$  Ma (MSWD of 1.6). An analytically indistinguishable concordant age of  $964 \pm 5.1$  Ma with an MSWD of 6.6 was calculated and is shown on Figure 18C.

The simplest interpretation of the data summarized above is that an older rock experienced several generations of zircon growth associated with Grenville and later metamorphic events (Figure 19). Thus the age of the rock is taken as ca.  $1170 \pm 8.5$  Ma with the addition of zircon rims at  $1026.8 \pm 4.3$  Ma and discrete pegmatitic or hydrothermal zircon at  $964 \pm 5.1$  Ma.



B.



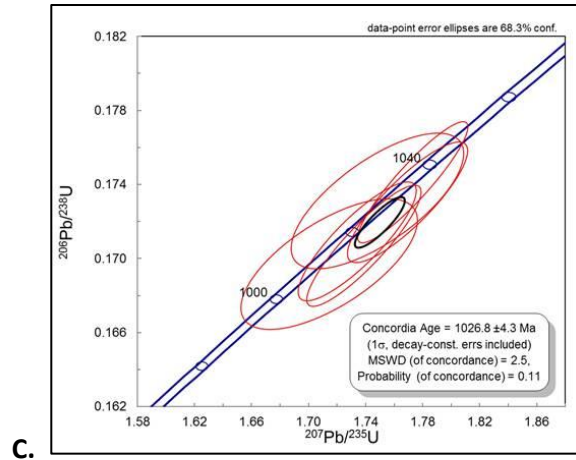


Figure 18. Geochronological results from a mineralized vein sample with magnetite from the Hogan Camp mine area. A. A total of 20 analyses are displayed on a concordia diagram and show two distinct groupings. B. A concordia diagram showing the concordant age of  $1170 \pm 8$  Ma (filled circle). C. Concordia diagram showing the concordant age (black ellipse) calculated from six zircon analyses.

### Ar/Ar thermochronology

Gates et al. (2001) reported on Ar/Ar thermochronology for mineralized brittle-ductile zones in the western Hudson Highlands. A summary of that work is included here. The Ar/Ar thermochronology was completed on hornblende and biotite samples from the mineralized rocks in the Hogencamp mine area. The samples analyzed at the Ar/Ar thermochronology lab at Massachusetts Institute of Technology, using standard step-wise heating techniques. Two hornblende and one biotite from the gangue minerals produced ages of  $914 \pm 3.6$  Ma,  $922 \pm 3.4$  Ma, and  $840 \pm 5.0$  Ma, respectively. While hornblende and biotite from an undeformed pegmatite within the mineralized vein produced ages of  $923 \pm 2.8$  Ma and  $794 \pm 3.0$  Ma. The relatively tight cooling ages for the mineralized and pegmatite hornblende suggest a genetic tie between the two with both mineralization and pegmatite crystallization occurring about the same time. Gates et al. (2001) inferred a very slow cooling rate from these results, however, the 45 Ma difference in the biotite cooling temperatures are perplexing suggesting problems with the results.

## COMPARATIVE GEOCHEMISTRY

There is a discrepancy in the overall results of the zircon geochronology from the lithotectonic units. Figure 19 summarizes the U-Pb ages, superimposed on the major tectonic events of the Grenville Province (after River, 2008). The detrital zircon cores produced ages that predate the Elzevirian Orogeny, and the rims appear to have grown during the Ottawa Orogeny.

The granitic gneiss sample of the Indian Hill shear zones produced a range of zircon core ages that span the Shawinigan Orogeny in addition to some metamorphic rims that grew toward the end of the same event. Additionally, that sample produced zircon rim ages that overlap with the Ottawa Phase of the Grenville Orogeny. It appears that rock bodies that are currently juxtaposed contain zircons that produced very different histories. Therefore, we decided to examine the geochemistry of these units in detail to possibly explain this discrepancy.

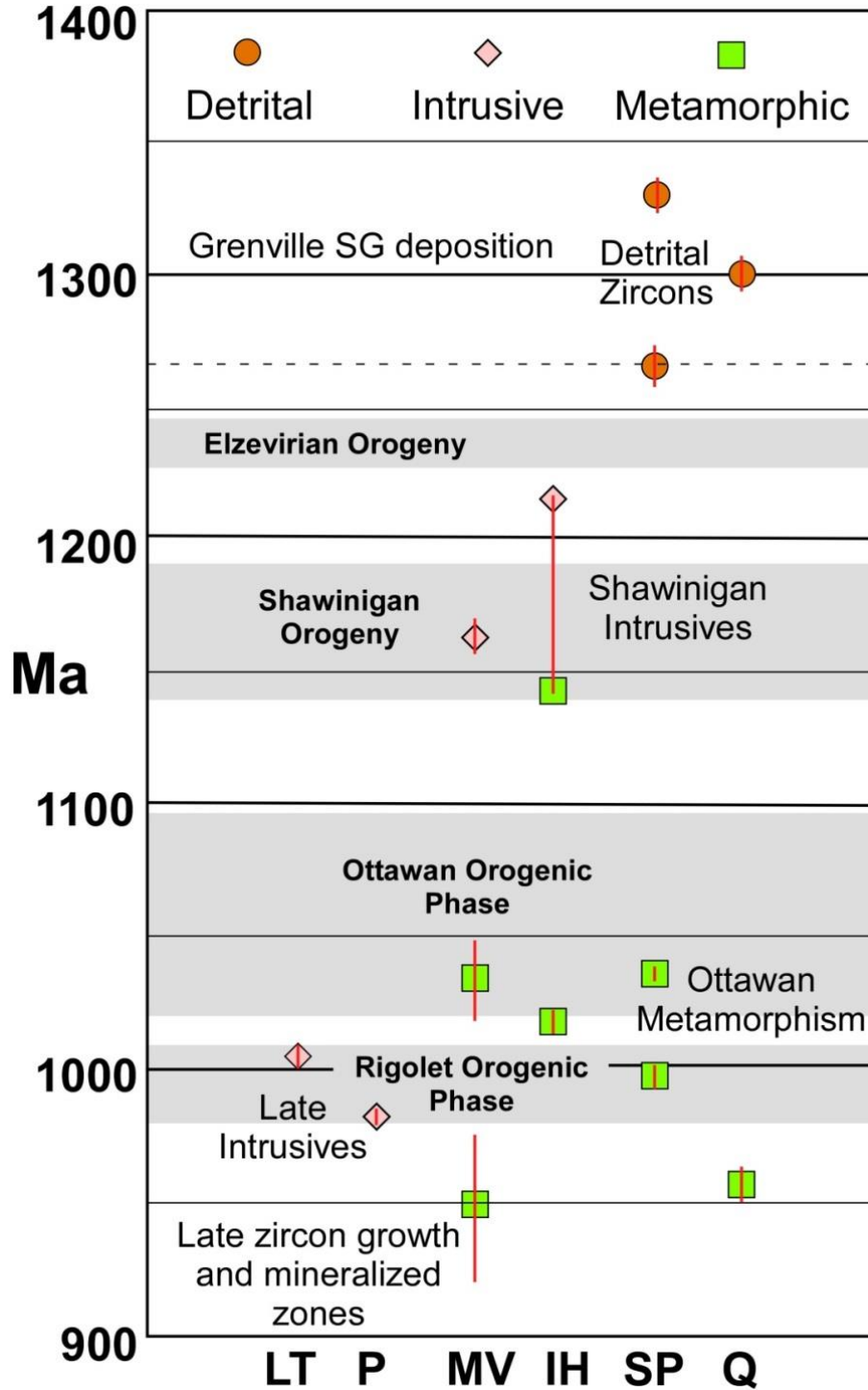


Figure 19. Summary of zircon U-Pb geochronology. Lake Tioroti (LT-diorite), P-pegmatite, Mineralized vein (MV-magnetite vein), Granitic gneiss within the Indian Hill shear zone (IH-granitic gneiss), Metasedimentary rocks (SP-semi-pelitic gneiss, Q-quartzite). Gray domains denote orogenic events and phases in the Canadian Grenville Province (after River, 2008).

Suites (ten samples each) of rock samples were selected from the sequence of metapelitic and metapsammitic gneisses, and from the granitic gneiss, and analyzed for whole rock major oxide and trace element compositions. The granitic gneiss is strongly deformed but reasonably homogeneous and most likely has a plutonic origin. In addition, rock samples from the metasedimentary lithofacies ranging in lithology from pelitic gneiss to quartzite were collected near Bear Mountain. The metasedimentary rocks range from 71.88 to 91.54 % SiO<sub>2</sub>. This is consistent with the interpretation that these rocks have a supracrustal origin. In fact, some of the supracrustal rocks are so enriched in silica that the role of the concentration of quartz during weathering is indisputable. The granitic gneiss samples range from 64.54 to 71.87% SiO<sub>2</sub>. This range is consistent with a granite origin for this gneiss body.

Igneous rocks can be subdivided based on the trend of a given related suite on an alkali-iron-magnesium (AFM) plot. Figure 20 displays both suites of geochemical analyses and shows a clear distinction in their trends. The granitic gneiss samples plot along the tie line between alkalis and iron, indicating an iron enrichment trend. This type of trend is seen in granitic rocks of anorogenic or "A"-type affinity such as the granitic members of the Anorthosite-mangerite-charnockite-granite or AMCG suite in the Adirondacks and elsewhere in the Grenville Province. Although the second suite of rocks are interpreted as metasedimentary in origin, it is also instructive to examine their trend on the AFM plot as a signature of their source terrane. Figure 20 shows a calc-alkaline trend for these rocks, suggesting derivation by erosion of an arc terrane.

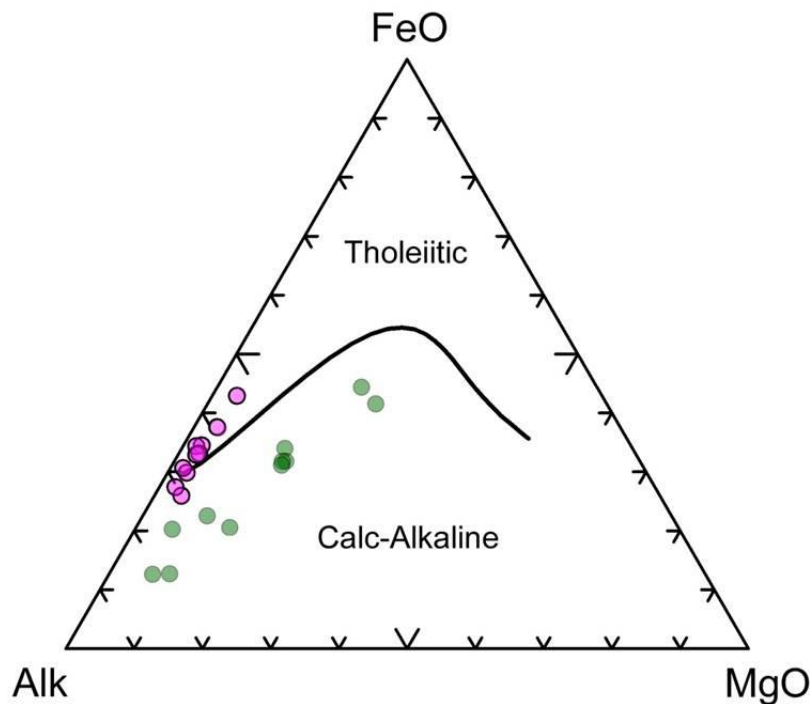


Figure 20. AFM diagram after Irvine and Barager (1971) showing samples of the granitic gneiss from the Indian Hill shear zone (pink or dark circles) and the Supracrustal sequence (green or pale). The granitic gneisses show a strong iron differentiation trend similar to granitic members of the Anorthosite-Mangerite-Charnockite-Granite (AMCG) suite in the Adirondacks and elsewhere. The supracrustal rocks show a calc-alkaline trend suggesting derivation from arc-related volcanic and/or plutonic rocks.

Examination of the rare earth element concentrations normalized to the Post-Archean Australian Shale (PAAS) composite of Taylor and McLennan (1985) provides insight into the origin of the two suites (Figure 21). Comparison of the REE trends shows no overlap in concentration and some distinct differences in patterns between the two suites. The granitic gneiss lies above “1” for each of the REE with several samples close to an order of magnitude more concentrated than PAAS. In addition, a distinctly negative europium anomaly can be seen on the diagram. This is characteristic of a fractionated felsic igneous rock from which plagioclase feldspar has been separated. The metasedimentary rock samples lie between “1” and “0.1” on the same diagram and approximately half of the samples have a strongly positive europium anomaly. The lower concentrations of REE is consistent with a detrital origin for the suite and can readily be explained by dilution by greater amounts of detrital quartz in arenaceous rocks. Quartz contains little or no trace elements including the REEs, so high silica clastic detrital rocks typically have lower REEs and other trace elements than more mud-rich rocks. The positive europium anomaly shown by several samples of the metasedimentary rocks indicates erosion of plagioclase-rich rocks that would be associated with an arc terrane.

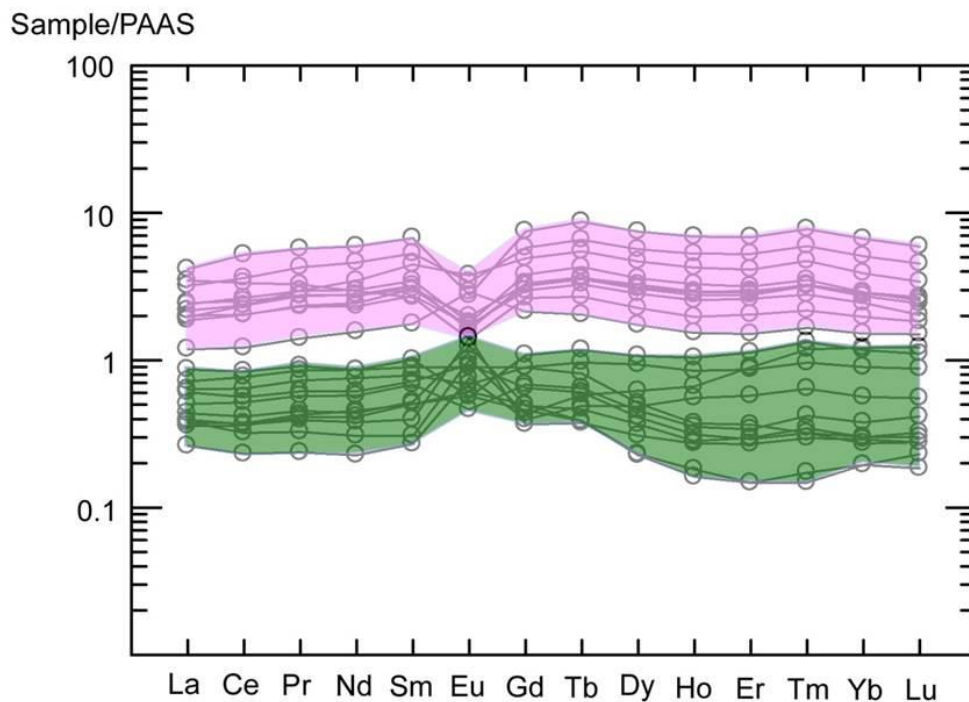


Figure 21. Rare earth element spidergram showing samples from the Indian Hill granitic gneiss (top field) and the supracrustal rocks (lower field). The rare earth element concentrations are normalized by the Post-Archean Australia Shale (PAAS) composite after Taylor and McLelland (1985). Major differences include the greater concentration of rare earth elements in the granitic gneisses and a negative, rather than positive, Europium anomaly. The concentration and pattern of the supracrustal rocks suggests dilution by quartz ( $\text{SiO}_2$  up to 91.45%) and erosion of a plagioclase-rich terrane.

Tectonic discrimination diagrams have found widespread utility in evaluating the setting of a variety of igneous rocks over the past several decades. Application to ancient orogenic settings and highly metamorphosed rocks may be useful particularly when other factors are considered along with the

discrimination diagrams. In Figure 22 the data from both suites of rocks is plotted on a discrimination diagram that uses Rb concentrations plotted against the sum of Y and Nb to subdivide granites into four fields. The granitic gneiss samples plot in the Within Plate Granite (WPG) field confirming their trace element signature is also consistent with an “A”-type origin. The metasedimentary rock samples plot within the Volcanic Arc Granitic (VAG) field consistent with other data suggesting the metasedimentary sequence was derived from the erosion of an arc terrane.

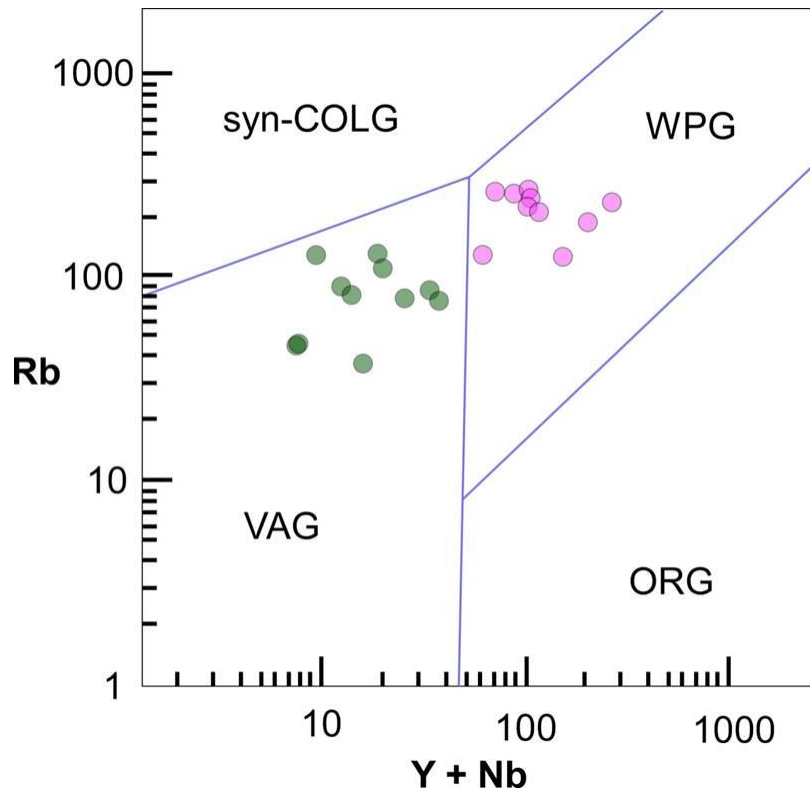


Figure 22. Rb versus Y + Nb tectonic discrimination diagram showing samples from the granitic gneisse (WPG field) and the supracrustal sequence (VAG field) after Pearce et al. (1984). The results are consistent with the granitic gneisses having an “A” type protolith and derivation of the supracrustal rocks by erosion of an arc terrane.

Finally, in Figure 23 both suites are plotted on a discrimination diagram designed to distinguish between the sources of granites. Based on the concentration of Zr versus Ga and Al the field is subdivided into an “A”-type granite field and one that combines both sedimentary (S-type) and igneous (I-type) granites. As is shown in the figure, the granitic gneiss samples fall exclusively within the upper right hand corner where “A”-type granites plot, whereas the metasedimentary rock samples plot within the S & I type fields. This suggests immobile trace elements can be used to differentiate the ultimate source region of both spots.

Geochemical investigation indicates that the granitic gneisses are chemically consistent within narrow limits and have the typical major and trace element signature found in “A”-type granites. They show a strong iron enrichment trend on the AFM diagram and fall within the with-in plate or “A”-type fields on discrimination diagrams. They show an enriched in REE over PAAS and have a negative europium

anomaly. Both of these characteristics are believed to be due to fractionation and the enrichment of trace elements due to their felsic composition and possibly the extent of partial melting of their source. Although the zircon systematics of these rocks defy a simple explanation, the age of the zircon cores is consistent with timing of "A"-type or AMCG granite intrusion in the Adirondacks and Grenville Province. This magmatism began about ca. 1185 Ma and continued to at least 1150 Ma elsewhere and perhaps in the Hudson Highlands as well.

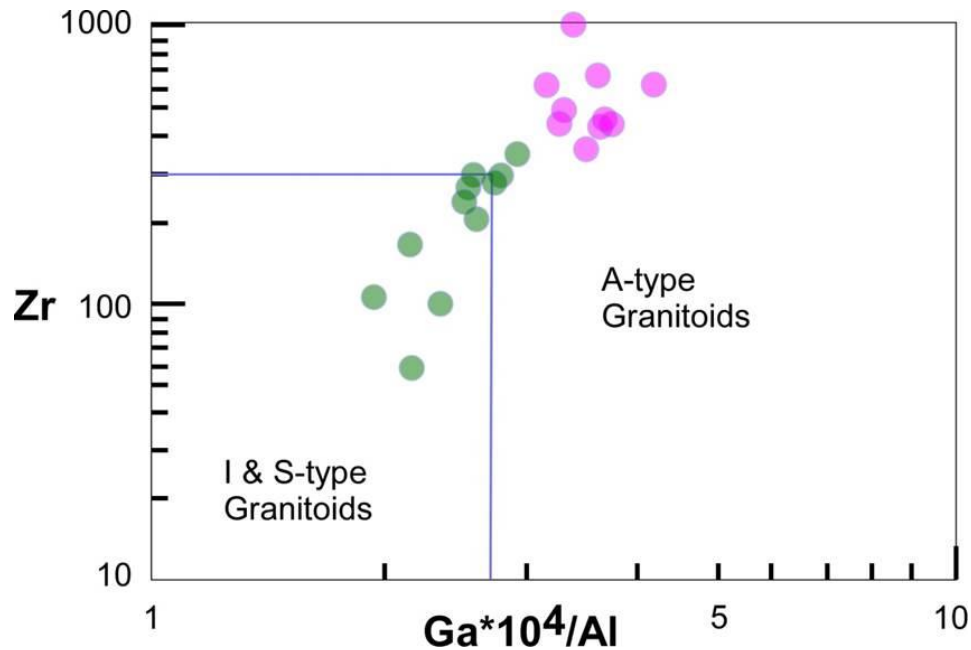


Figure 23. Tectonic discrimination diagram showing Zr vs. Ga\*1000/Al concentrations for the granitic gneisses (A-type Granitoid field) and the supracrustal sequence (cluster in the I & S-type Granitoid field with two samples in the A-type field) after Whalen et al. (1987).

Rocks of the metasedimentary lithofacies have chemical characteristics indicative of a supracrustal sequence ranging from pelitic to quartz-rich. In addition, the major and trace element characteristics indicate they were derived from an arc terrane. They have substantially lower REE than the PAAS composite and this reflects the inclusion of coarser-grain clastic rocks in the suite. On the AFM plot and tectonic discrimination diagrams they show a calc-alkaline trend and arc related geochemistry. The metasedimentary rocks are interpreted to be part of the Grenville Supergroup which was deposited in a series of back-arc basins (Gundersen, 1986; Gates et al., 2001) between 1250-1300 Ma. A viable source for the clastic material they contain would be an arc or arc fragments of the widespread Dysart-Mt. Holly Complex ranging in age from 1300-1350 Ma and/or local metavolcanic equivalents.

## TECTONIC CONCLUSIONS

1. The lithotectonic units in the western Hudson Highlands represent a complex sequence of deposition, volcanism and intrusions, superimposed by multiple regional deformation events that occurred deep in the crust. Detrital zircons from two separate bodies of metasedimentary rocks yielded provenances ranging in age from 1.2 to 2.7 Ga. The younger detrital ages are consistent with the Grenville Supergroup, however the wide range of older ages with Archean sources. Gates et al. (2006) proposed

that the range of ages suggests deposition in a passive margin with a possible Amazonian contribution. It was suggested by Gates et al. (2006) that the Archean ages may reflect an Amazonian source contribution to the detrital material. As well, this interpretation is supported by the metasedimentary lithotectonic rock assemblage including quartzite, marble, calcsilicate and pelities is consistent with this interpretation.

2. The metavolcanic and metavolcaniclastic rocks most likely represent the remains of a volcanic arc, including the granitic intrusive rocks that are now granitic gneiss. The granitic gneiss body yielded a range of zircon ages of 1235 to 1159 Ma, suggesting that the granite intruded before or during the Shawinigan Orogeny, but the geochemistry suggests the body is related to the A-type suite of plutons associated with the AMCG rocks of the Adirondacks and Grenville Province. The sample of granitic gneiss is from the Indian Hill shear zone, and the span of ages is attributed to subsequent mylonitic deformation and metamorphism.

3. Gorrington et al. (2003), suggested that the Lake Tioroti diorite and other minor granitic bodies in the western Hudson Highlands were associated with localized transtensional deformation within the transcurrent shear system. The age of the Lake Tioriti diorite is 1008 Ma, and the shear zone fabric occurs along the margin of the body, suggesting that shearing and intrusion were linked. This is the same structural relationship that was observed for the granite sheets that occur in the hinges of transpressional folds between the dextral shear zones. The intrusion of igneous bodies during dextral shearing requires elements of dilation, but the location of the bodies in the cores of upright folds suggests that the bodies migrated to domains of vertical escape in an overall transpressional tectonic environment. Constrained by cross cutting pegmatite, the high-grade ductile dextral transpression in the western Hudson Highlands was over by 980 Ma. But, lower temperature brittle-ductile deformation in the same shear system continued and was accompanied by mineralization.

FIELD GUIDE AND ROAD LOG

Meeting Point: This field trip begins at the upper parking lot for the Sterling Forest visitor center within the Sterling Forest State Park.

Meeting Point Coordinates: 41.197°N, 74.256°W

Meeting Time: 9:00AM

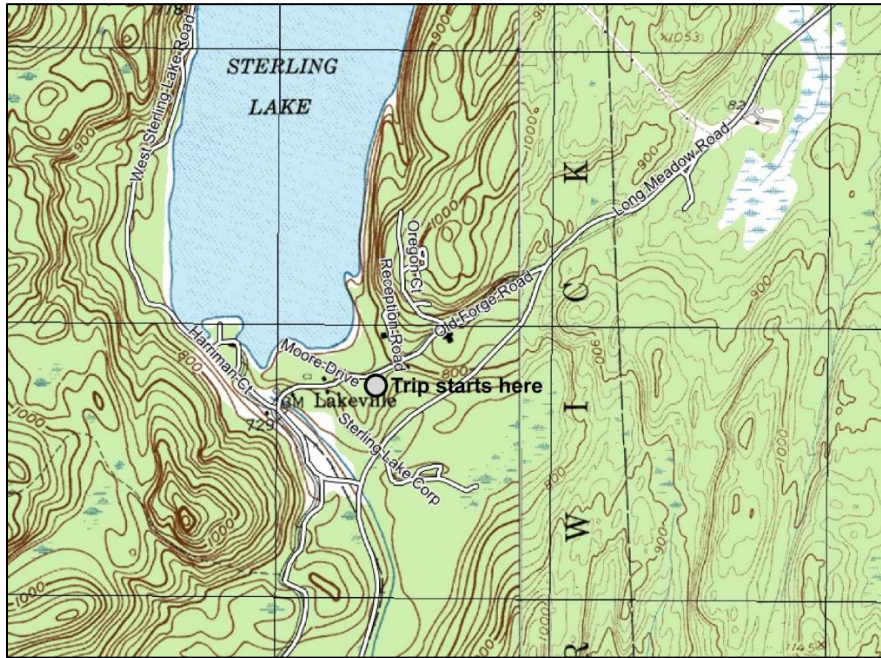


Figure 24. Topographic map showing the starting location for the field trip near the Sterling Forest visitor center on Old Forge Road.

Distance in miles (km)		
Cumulative	Point to point	Route Description
0.0 (0.0)	0.0 (0.0)	Turn right when exiting the parking lot onto Old Forge Road.
0.5 (0.8)	0.5 (0.8)	Turn right onto Long Meadow Road and follow the intersection with Route 72.
4.7 (7.6)	4.2 (0.8)	Turn left onto Route 72.
6.0 (9.7)	1.3 (2.1)	Turn left onto Eagle Valley Road.
6.1 (9.8)	0.1 (0.2)	Park in the gravel lot on the left side of road. Walk about 0.1 miles along the road until you reach the dirt road under the power line. Follow the power line road about 0.1 miles up-hill to the left. Stop 1 is located under the first tower that you encounter along the dirt road.



Stop 2. Metasedimentary Lithofacies, Seven Lakes Drive, Sloatsburg, NY

Location Coordinates: (41.190°N, 74.143°W)

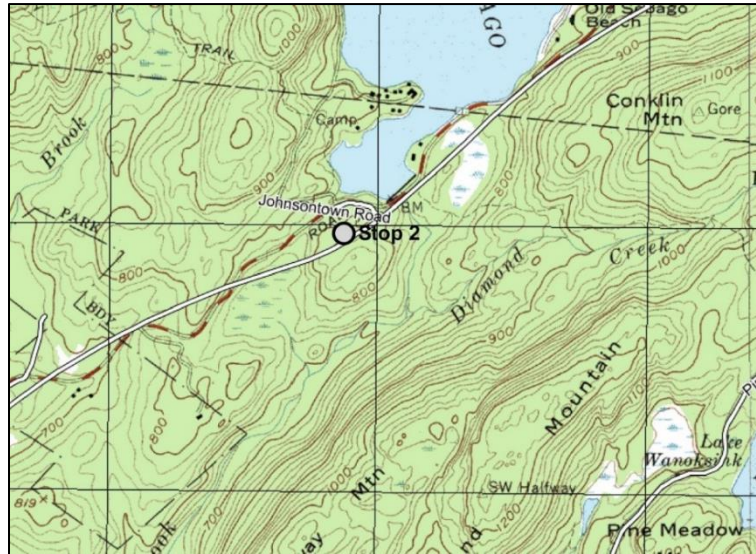


Figure 26. Topographic map showing the location of Stop 2 on Seven Lakes Drive.

The rocks at this stop include sillimanite-garnet-biotite gneiss, and graphite-pyrite bearing metapsammitic gneiss. The presence of sulfides accounts for the rusty weathered outcrop surface. The dominant foliation in this gneiss is the regional S1 with minor crenulations and open folds that are subparallel to mineral lineations. Gates et al. (2006) interpreted these rocks to represent low energy sedimentary deposits in a restricted marine basin.



Figure 27. Outcrop photograph of interlayered pelitic, semi-pelitic and psammitic gneiss bearing abundant sulfides.

NYSGA: Geologic Diversity in NYC

Distance in miles (km)		Route Description
Cumulative	Point to point	
15.9 (25.6)	3.7 (6.0)	Approach Kanawauke Circle from the south. Proceed north on Seven Lakes Dr.
18.4 (29.6)	2.5 (4.0)	Pass the Tioriti diorite outcrop on left. Refer to Gates et al. (2002); Gorrington et al. (2003); and Gates et al. (2006) for description of this outcrop. This trip will proceed north.
19.2 (30.9)	0.8 (1.3)	Approach Tioriti Circle from the south. Proceed north on Seven Lakes Drive.
22.9 (36.9)	3.7 (6.0)	Approach the intersection with Route 6. Seven Lake Drive merges with Route 6. You will exit the circle half way around and continue east until the two roads split. Take the exit for Seven Lakes Drive, toward Bear Mountain Park.
23.7 (38.1)	0.8 (1.3)	At the end of the exit road, park on the wide shoulder to Seven Lakes Drive. Carefully walk back on the exit road and onto Route 6 until you read the end of a very long outcrop on the left. This is the beginning of Stop 3. Examine the outcrop as you slowly proceed back to the vehicles.

Stop 3. Metasedimentary Lithofacies, Palisades Interstate Parkway, Doodletown, NY

Location Coordinates: (41.307°N, 74.028°W)

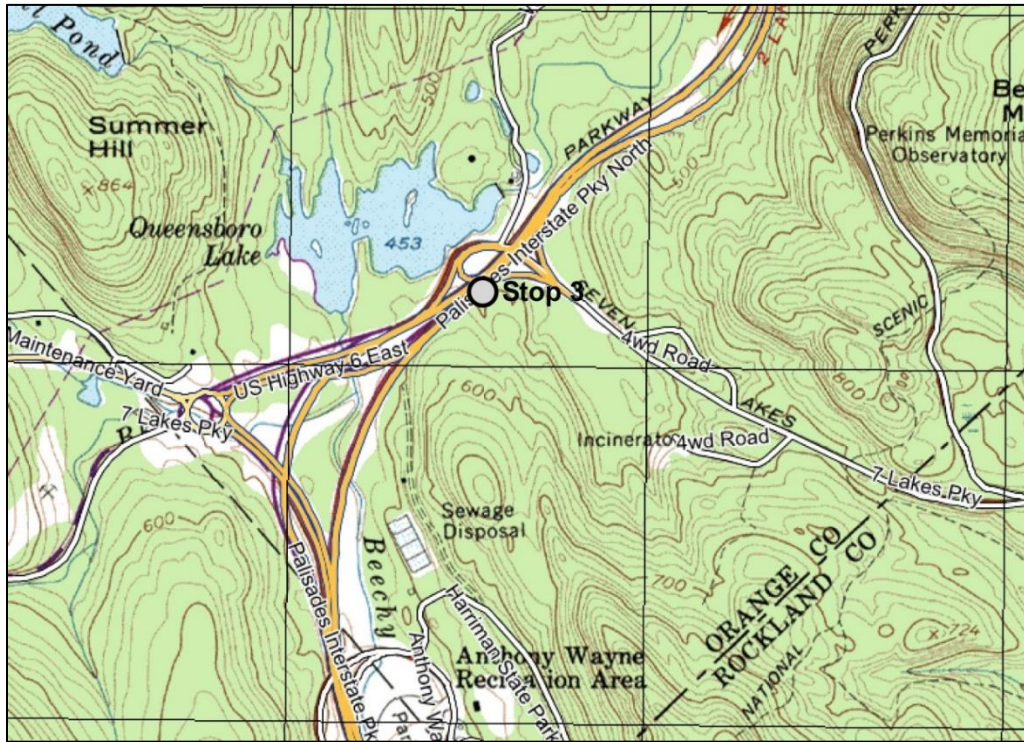


Figure 28. Topographic map showing the location of the supracrustal rocks at Stop 3.

An extensive sequence of interlayered quartzite, semi-pelitic gneiss and pelitic gneiss outcrop at Stop 3 along the Palisades Interstate Parkway. The compositional layering most likely represents the compositional variation of the sedimentary protoliths. The pelitic layers contain biotite, garnet, sillimanite and K-feldspar, while the quartzite layers contain primarily recrystallized quartz and K-feldspar and garnets. Samples from this outcrop were analyzed to characterize the geochemistry of this unit, and one sample of quartzite was used for U-Pb geochronology. The results of this work is discussed above.

Distance in miles (km)		
Cumulative	Point to point	Route Description
31.6 (50.7)	7.8 (12.6)	Back track on Seven Lakes Drive to the Kanawauke Circle in Harriman State Park. Turn right onto Kanawauke Road.
32.1 (51.7)	0.6 (1.0)	Optional stop. Turn left into the parking lot. Walk 0.4 miles farther on Kanawauke Road to examine an outcrop of the Metavolcanic Lithofacies. Refer to the NYSGA 2001 Guidebook, Trip 3, Stop 3. Proceed west on Kanawauke Dr.
36.8 (59.2)	4.7 (7.6)	Kanawauke Drive will pass under the NY Thruway and end at a stop sign. Proceed straight onto Route 17A.
37.5 (60.4)	0.7 (1.1)	Park on the wide shoulder of Route 17A. There are abundant outcrops on the north side of the highway. This is Stop 4.

Stop 4. Granitic Gneiss of the Indian Hill Shear Zone, Route 17A, Tuxedo Park, NY

Location Coordinates: (41.234°N, 74.193°W)

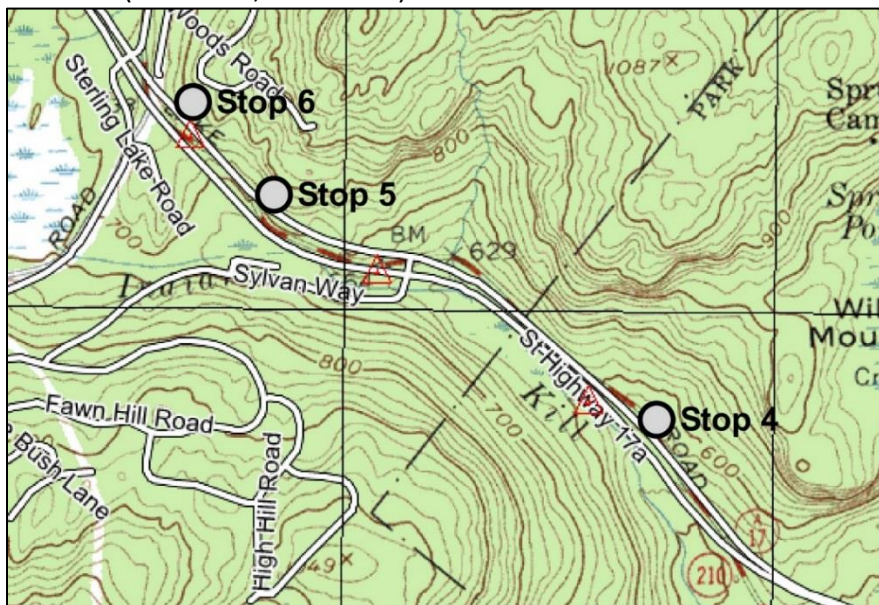


Figure 29. Topographic map showing the locations of Stops 4, 5 and 6 along Route 17A.

There are numerous outcrops of granitic gneiss along the west bound lanes of Route 17A (Figure 29). Stop 4 is a series of outcrops within the first kilometer along the road. This area is underlain by highly deformed granitic gneiss, and a complete cross section of the Indian Hill ductile shear zone (Allers et al., 2001). The granitic gneiss contains a steeply east dipping penetrative foliation defined by recrystallized planar aggregates of quartz, K-feldspar and plagioclase, with subhorizontal mineral lineations. In places, there is well developed S-C fabric, and relict feldspar grains forming asymmetric augen. Using oriented samples, kinematic analysis of these macroscopic structures reveals a dominant dextral shear sense. In places, the foliation is disrupted by minor leucosomes, forming asymmetric boudins (Figure 9) with the same shear sense. Commonly, there are amphibolite layers ranging from a few cm to a meter wide within the granitic gneiss. The amphibolite layers are internally foliated with boundaries that are parallel to the penetrative foliation in the granitic gneiss. One thicker layer has an array of granite-filled en-echelon veins that also consistent with dextral shear (Figure 30).

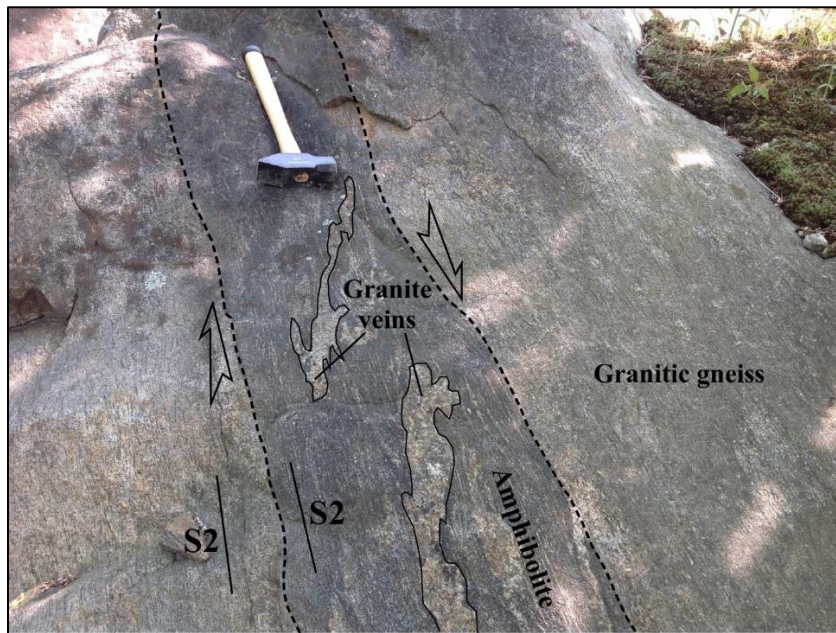


Figure 30. Outcrop photograph of strongly foliated granitic gneiss with an amphibolite layer that has dextral en-echelon granite veins. View is looking into the ground and the hammer handle trends approximately 215 degrees.

Distance in miles (km)		Route Description
Cumulative	Point to point	
38.0 (61.2)	0.5 (0.8)	Proceed west on Route 17A. Park on wide shoulder just past the blind curve. There are a pair of outcrops on both sides of the highway. Be especially cautious when crossing the double lakes of Route 17A. This is Stop 5.

Stop 5. Granitic Gneiss and Pegmatite, Route 17A, Tuxedo Park, NY

Location Coordinates: (41.238°N, 74.202°W)

Stop 5 is a series of outcrops that are on both sides of the west bound lanes of Route 17A. At this location, the granitic gneiss of Stop 4 is cross cut by a pegmatite that is several meters thick. The contact is well exposed on both sides of the highway, however for those of you that are allergic to poison ivy, it is recommended that you carefully cross the highway to view the pegmatite –granitic gneiss contact on the south side of the highway. The pegmatite contains typical K-feldspar and quartz in a addition to large hornblende crystals that form a nearly subhorizontal lineation that relects growth direction. This location is where samples were collected for U-Pb zircon geochronology previously discussed in this field guide.

---

Distance in miles (km)		
Cumulative	Point to point	Route Description
38.2 (61.5)	0.2 (0.3)	Proceed west on Route 17A and park on the wide shoulder. This is Stop 6.

---

Stop 6. Calcsilicate Gneiss, Route 17A, Tuxedo Park, NY

Location Coordinates: (41.240°N, 74.205°W)

The granitic gneiss is in sharp contact with calcsilicate gneiss between Stop 5 and 6 along Route 17A. The calcsilicate gneiss contains plagioclase, quartz, diopside and epidote in the prominent dark layers that are strongly foliated. Lighter layers are leucosomes of K-feldspar and quartz that are parallel to the penetrative foliation (Figure 31). In most places, and especially at this location, the calcsilicate gneiss occurs as a minor migmatite. Typically, the calcsilicate gneiss is interlayered with other metasedimentary lithologies such as pelites, psammites and marble. But, this body is one of the thickest, reaching upward of several hundred meters and was traced for more than 5 kilometers to the northeast along the margin of the granitic gneiss. The foliation in this calcsilicate appears to be composite where S2 (gneissocity) has been transposed parallel to the local shear zone (S2).



Figure 31. Outcrop photograph of calcisilicate gneiss with the typical melanosomes of diopside-quartz-plagioclase- epidote and leucosomes of K-feldspar-quartz.

Distance in miles (km)		
Cumulative	Point to point	Route Description
38.8 (62.4)	0.6 (1.0)	Turn left onto Long Meadow Road.
39.6 (63.7)	0.8 (1.3)	Turn right onto Ironwood Drive.
40.8 (65.7)	1.2 (1.9)	Proceed to the end of Ironwood Drive and park. Walk the dirt road to the about 0.2 miles to the large outcrops of granite under the power-line tower. This is Stop 7.

**Stop 7. Bare Mountain Granite, Ironwood Drive, Tuxedo Park, NY**

Location Coordinates: (41.232°N, 74.237°W)

A series of granite sheets underlie the hills on the north and south side of the Ironwood Drive valley (Figure 33). The sheets range in thickness from a few meters upward of several hundred meters. Note the serrated topography on the south flank of Hogback Mountain in the topographic map above. Each of the promontories on the side of the mountain is underlain by the more resistant granite. The granite at Bare Mountain is one of the thicker granite sheets. Excellent outcrops occur on the western flank of Bare Mountain and for those interested in a good climb it would be worth the time to scale the face to examine a cross section of the granite. However, the same granite is readily accessible along the dirt road that follows the powerline. At this location, the granite is pink to white, leucocratic, containing quartz, K-feldspar and plagioclase with only trace amount of biotite or hornblende. In places, there are K-feldspar megacrysts upward of 10 cm in diameter. Although not exposed at this location, the contact with the local country rock is sharp, but the granite has a weakly to moderately developed mylonitic foliation.



Figure 32. Topographic map showing the location of the Bare Mountain granite at Stop 7 at the end of Ironwood Drive in the Sterling Forest.



Figure 33. Bare Mountain granite outcrops at Stop 7 with pressure release sheet joints.

Distance in miles (km)		
Cumulative	Point to point	Route Description
42.0 (67.6)	1.2 (1.9)	Proceed back on Ironwood Dr. to Long Meadow Rd. Turn left.
44.3 (71.3)	2.3 (3.7)	Optional stop. This is an outcrop of a smaller granite sheet. Refer to the 2003 NYSGA Guidebook, Appendix A, Trip A6, Stop 2 for details (Gorring et al., 2003).
44.4 (71.5)	0.1 (0.2)	Turn right onto Old Forge Road and proceed to the parking lot.
44.8 (72.1)	0.4 (0.6)	Parking lot where the trip started.

## REFERENCES CITED

- Allers, T., Valentino, D., Gates, A. and Chiarenzelli, J., 2001, Structural analysis of the Indian Hill shear zone, Hudson Highlands, NY, Geological Society of America, Abstracts with Programs, v. 33, p. 79.
- Chiarenzelli, J., Kratzmann, D., Selleck, B., and de Lorraine, W., 2015, Age and provenance of Grenville Supergroup rocks, Trans-Adirondack Basin, constrained by detrital zircons: *Geology*, v. 43; no. 2; p. 183–186.
- Dallmeyer, R. D., 1974, Metamorphic history of the northeastern Reading Prong, New York and Northern New Jersey, *Journal of Petrology*, v. 15, p. 325-359.
- Gates, A. E. and Valentino, D. W., 2011, Bedrock geology of the Highlands, *in* (ed. Lathrop, R. G., Jr.) *The*

*NYSGA: Geologic Diversity in NYC*

- Highlands, Critical Resources, Treasured Landscapes, Rutgers University Press, New Brunswick, NJ, p. 9-25.
- Gates, A. E., Valentino, D. W., Gorrington, M. L. and Hamilton, M., 2001, The assembly of the Supercontinent Rodinia in the western Hudson Highlands, New York State Geological Association, Field Trip Guidebook, v. 73, p. 174-204.
- Gates, A. E., Valentino, D. W., Gorrington, M. L., Tern, E. R. and Chiarenzelli, J. R., 2006, Rodinian collision and escape tectonics in the Hudson Highlands, New York, Geological Society of America, Field Guide 8, p. 65-82.
- Gorrington, M. L., Valentino, D. W., Solar, G. S. and Gates, A. E., 2003, Late Ottawa ductile shearing and granitoid emplacement in the Hudson Highlands, NY, New York State Geological Association, Field Trip Guidebook, v. 75, Appendix A., p. 1-27.
- Gundersen, L.C., 1986, Geology and geochemistry of the Precambrian rocks of the Reading Prong, New York and New Jersey - Implications for the genesis of iron-uranium-rare earth deposits, In USGS Research on Energy Resources - 1986 Programs and Abstracts (Carter, L.M.H., ed.), U.S.G.S. Circular 974, 19 p.
- Irvine, T.N., and Baragar, W.R.A., 1971, A guide to the chemical classification of the common volcanic rocks: Canadian Journal of Earth Sciences, v. 8, p. 523-548.
- Linguanti, C., Valentino, D., Gorrington, M. and Gates, A., 2011, Synorogenic emplacement of granite sheets, Hudson Highlands, New York, Geological Society of America, Abstracts with Programs, v. 43, p. 149.
- Peck, W., Selleck, B., Wong, M., Chiarenzelli, J., Harpp, K., Hollocher, K., Lackey, J., Catalano, J., Regan, S., and Stocker, A., 2013, Orogenic to postorogenic (1.20–1.15 Ga) magmatism in the Adirondack Lowlands and Frontenac terrane, southern Grenville Province, USA and Canada: Geosphere, v. 9, p. 1637-1663.
- Rivers, T., 2008, Assembly and preservation of lower, mid, and upper orogenic crust in the Grenville Province—Implications for the evolution of large hot long-duration orogens, Precambrian Research, v. 167, p. 237-259.
- Stilwell, S., 2006, Geothermometry of pelitic rocks from the western Hudson Highlands, New York, State University of New York at Oswego, B.S. Thesis, 72 p.
- Pearce, J.A., Harris, N.B.W., and Tindle, A.G., 1984, Trace element discrimination diagrams for the tectonic interpretation of granitic rocks: Journal of Petrology, v. 25, p. 956-983.
- Taylor S. R., McLennan S. M., 1985, The continental crust: its composition and evolution. Blackwell Scientific Publication, Carlton, 312 p.
- Thomas, J., Valentino, D. and Gates, A., 2001, Structural control on the intrusion of granite sheets in the Hudson Highlands, NY, Geological Society of America, Abstracts with Programs, v. 33, p. 29.
- Whalen, J.B., Currie, K.L., and Chappell, B.W., 1987, S-type granites: geochemical characteristics, discrimination and petrogenesis. Contributions to Mineralogy and Petrology, v. 95, p. 407-419.